Development 130, 1605-1620

doi:10.1242/dev.00385

Developmental defects observed in hypomorphic anaphase-promoting complex mutants are linked to cell cycle abnormalities

Diane C. Shakes[1,*,†], Penny L. Sadler[2,*], Jill M. Schumacher[3], Maziar Abdolrasulnia[1] and Andy Golden[2]

[1]Department of Biology, College of William and Mary, Williamsburg, Virginia 23187, USA
[2]Laboratory of Biochemistry and Genetics, National Institute of Diabetes and Digestive and Kidney Diseases, National Institutes of Health, Bethesda, Maryland 20892, USA
[3]Department of Molecular Genetics, The University of Texas MD Anderson Cancer Center, Houston, TX, 77030 and Genes and Development Program, Graduate School of Biomedical Sciences, The University of Texas-Houston, Houston, TX 77030, USA
*These authors contributed equally to this work
†Author for correspondence (e-mail: dcshak@wm.edu)

Accepted 9 January 2003

SUMMARY

In *C. elegans*, mutants in the anaphase-promoting complex or cyclosome (APC/C) exhibit defects in germline proliferation, the formation of the vulva and male tail, and the metaphase to anaphase transition of meiosis I. Oocytes lacking APC/C activity can be fertilized but arrest in metaphase of meiosis I and are blocked from further development. To examine the cell cycle and developmental consequences of reducing but not fully depleting APC/C activity, we analyzed defects in embryos and larvae of *mat-1/cdc-27* mutants grown at semi-permissive temperatures. Hypomorphic embryos developed to the multicellular stage but were slow to complete meiosis I and displayed aberrant meiotic chromosome separation. More severely affected embryos skipped meiosis II altogether and exhibited striking defects in meiotic exit. These latter embryos failed to produce normal eggshells or establish normal asymmetries prior to the first mitotic division. In developing larvae, extended M-phase delays in late-dividing cell lineages were associated with defects in the morphogenesis of the male tail. This study reveals the importance of dosage-specific mutants in analyzing molecular functions of a ubiquitously functioning protein within different cell types and tissues, and striking correlations between specific abnormalities in cell cycle progression and particular developmental defects.

Key words: *mat-1/cdc-27*, Asymmetric cell divisions, Meiosis, Cell cycle, APC/C, *Caenorhabditis elegans*

INTRODUCTION

The anaphase-promoting complex or cyclosome (APC/C) is an evolutionarily conserved, multi-subunit E3 ubiquitin ligase that irreversibly drives cells through and subsequently out of mitosis (Harper et al., 2002; Peters, 2002). Like other E3 ubiquitin ligases, the APC/C functions by poly-ubiquitinating its specific target proteins, thus marking them for destruction by the 26S proteasome. Models of APC/C function, based largely on studies in unicellular eukaryotes, suggest that the APC/C acts at two key points during mitosis. Initially, the APC/C drives cells from metaphase to anaphase by poly-ubiquitinating securin, the inhibitory binding partner of separase (Cohen-Fix et al., 1996; Funabiki et al., 1996b). Liberated separase can, in turn, proteolytically cleave cohesin proteins between sister chromatids, thus enabling microtubule-associated forces to pull the separated sisters to opposing spindle poles (Uhlmann et al., 1999; Uhlmann et al., 2000). The APC/C then promotes mitotic exit by ubiquitinating the M-phase cyclins (reviewed by Morgan, 1999). More recently, the APC/C has been shown to function in separating paired homologs during meiosis I (Cooper et al., 2000; Davis et al., 2002; Furuta et al., 2000; Golden et al., 2000) and sister chromatids during meiosis II (Peter et al., 2001; Taieb et al., 2001). To date, SnoN, a negative regulator of TGFβ signaling (Stroschein et al., 2001; Wan et al., 2001) is the only documented non-cell cycle target of the APC/C. In contrast, SCF, the E3 ligase that drives the G1 to S transition, has a wide variety of non cell-cycle targets (reviewed by Deshaies, 1999; Hershko and Ciechanover, 1998).

Nonetheless, the APC/C is likely to have several other targets in addition to securin and the M-phase cyclins. For instance, the APC/C clearly regulates spindle and chromosome dynamics beyond disrupting sister chromatid cohesion since its known spindle-related substrates include Ase1 (Juang et al., 1997; Visintin et al., 1997) Aurora-A (Castro et al., 2002; Taguchi et al., 2002) and several specialized kinesins (Funabiki and Murray, 2000; Gordon and Roof, 2001). Recent studies have also implicated developmental roles for the APC/C during spore formation in yeast (Asakawa et al., 2001; Blanco et al., 2001) and embryonic axis formation in *C. elegans* (Rappleye et al., 2002). However, in the absence of identified developmentally relevant substrates, it is unclear whether the APC/C regulates these developmental processes directly or indirectly via its known cell cycle substrates.

Several features make *C. elegans* an excellent model system

not only for analyzing the role of the APC/C in cell cycle progression but also for investigating potential links between the cell cycle and development. For instance, the developmental impact of cell cycle mutants that truncate or alter the timing of cell lineages can be studied in the context of a known, invariant cell lineage and well-understood developmental signaling interactions (reviewed by Lambie, 2002). In fact, the late-developing everted vulva phenotype in *emb-30/apc-4* mutants, and presumably other APC/C mutants, has been shown to be associated with extended M-phase delays and variable lineage truncations within the vulva cell lineage (Furuta et al., 2000). In a different multicellular context, the *C. elegans* germline is a highly proliferative tissue, which like the germline and imaginal discs in *Drosophila*, is particularly sensitive to cell cycle defects (Albertson et al., 1978; Glover, 1989). Given that the 1000+ cells that compose the mature, syncytial germline arise from just two cells within hatching L1 larva (Hirsh et al., 1976), it is not surprising that many APC/C mutants develop severely reduced germlines due to mitotic defects (Furuta et al., 2000; Golden et al., 2000).

Lastly, the powerful combination of excellent cytology, well-established genetics and RNA interference (RNAi) methodology can be used to analyze how the APC/C functions at the cellular level to support cell cycle progression and development of the *C. elegans* zygote. The one-cell stage of these large, transparent embryos encompasses both meiotic divisions of the oocyte chromosomes and the subsequent events leading up to the first mitotic division. Thus, these zygotes can be used to study common but poorly understood modifications of the standard cell cycle including how cells transition between meiosis I (MI) and meiosis II (MII) in the absence of full M-phase exit (reviewed by Abrieu et al., 2001), and how cells exit meiosis II and enter pre-mitotic S phase in the apparent absence of G1 (King et al., 1994; Vidwans and Su, 2001). In *C. elegans*, meiotic exit is accompanied by a striking change in microtubule dynamics. During the meiotic phase, oocyte chromosomes segregate on small, anastral, acentriolar spindles (Albertson and Thomson, 1993), but, upon meiotic exit, the sperm centrosomes begin to nucleate microtubules as nearby cytoplasmic microtubules disappear (Clandinin and Mains, 1993). These developing sperm asters also specify the position of the embryonic posterior (Goldstein and Hird, 1996; O'Connell et al., 2000; Sadler and Shakes, 2000; Wallenfang and Seydoux, 2000) and thus microtubules may serve as a common link between cell cycle progression and the zygote's developmental program.

The role of the APC/C in the various cell cycle and developmental events of the one-cell *C. elegans* embryo is just beginning to be elucidated. When any one of several APC/C subunits is significantly depleted, the affected embryos experience both a cell cycle block in metaphase of meiosis I and a corresponding developmental block (Davis et al., 2002; Furuta et al., 2000; Golden et al., 2000; Kitagawa et al., 2002). To date, this metaphase I block has precluded the analysis of *C. elegans* APC/C functions in meiosis II, meiotic exit or the first mitotic division of the embryo.

Here, we demonstrate that *mat-1*, a gene known to be involved in meiosis I metaphase to anaphase transition (Golden et al., 2000), encodes the CDC27/APC3 subunit of the APC/C. To analyze late and possibly novel APC/C functions, we focused on specific hypomorphic defects exhibited by seven temperature-sensitive *mat-1* alleles grown under a variety of temperature-shift regimes. These studies, in conjunction with RNAi dosage studies and combinations of APC/C double mutants, demonstrate that different levels of APC/C activity result in distinct meiotic and post-embryonic phenotypes. Our analysis not only reveals new roles for the *C. elegans* APC/C in meiotic spindle dynamics, meiosis II chromosome separation, and meiotic exit, but it also extends our understanding of the male tail defects in APC/C mutants. Importantly, specific APC/C-related cell cycle defects were found to correlate with predictable and distinct developmental abnormalities suggesting that at least some of the previously reported developmental defects (Lyczak et al., 2002; Rappleye et al., 2002) might be secondary consequences of meiotic progression and exit abnormalities.

MATERIALS AND METHODS

Strains and genetic analysis

Six alleles of *mat-1* were isolated in a large-scale genetic screen for temperature-sensitive mutants that arrest during the MI metaphase to anaphase transition (Golden et al., 2000), while a seventh allele (*ye121*) was subsequently isolated in an independent screen for osmotically sensitive mutants (Rappleye et al., 2002). To facilitate the analysis of male phenotypes, genetic doubles of *mat-1* alleles were constructed with *him-5(e1490)* (V) or *him-8(e1489)* (IV); all male phenotypes were confirmed in *him*/+ strains.

Construction of double mutants and GFP lines

Doubly marked *mat-1(ax227ts); mat-x* or *mat-1(ax227ts); emb-x* strains were constructed as follows: *unc-38(x20) mat-1(ax227ts)* or *mat-1(ax227ts) dpy-5(e61)* L4 hermaphrodites were mated with N2 or *him-8(e1489)* males. Non-Unc and non-Dpy male progeny from these crosses were mated with L4 hermaphrodites of the following genotypes: *mat-2(or170ts) unc-4(e120)*, *mat-3(ax148ts) dpy-1(e1)*, *mat-3(or180ts) dpy-1(e1)*, *emb-27(g48ts) unc-4(e120)*, and *emb-30(g53ts) dpy-17(e164)*. Five to ten non-Unc or non-Dpy cross progeny were picked and from the next generation, the phenotypes of the DpyUnc double mutant animals were determined. In all cases, double mutant strains could be identified, though many of the double mutant strains could not be maintained. All of the above crosses were carried out at the permissive temperature of 15°C.

For the *mat-1* allele *ax212ts*, double mutants were constructed with an unmarked *ax212ts* allele. *mat-1(ax212ts); him-5(e1490)* males were mated with marked L4 hermaphrodites listed above. Non-Unc or non-Dpy F_1 progeny were picked, and then 16 F_2 Unc or Dpy animals were picked to separate plates (thus homozygous for the second *mat* or *emb* loci). One quarter of such animals should also be homozygous for *ax212ts*. These plates were examined for the presence of candidate double mutants. Again, these experiments were carried out exclusively at the permissive temperature (15°C).

For the *mat-1(ye121ts); mat-3(or180ts)* double mutant, *mat-1(ye121ts); him-8 (e1489)* males were mated with *mat-3(or180ts) dpy-1(e1)* L4 hermaphrodites. From the progeny of non-Dpy F_1 animals, 51 F_2 Dpy Mat-3 animals were picked to separate plates. One quarter of such animals should also be homozygous for *ye121ts*. These plates were examined for the presence of candidate double mutants at the permissive temperature. The same cross was performed and F_2 embryos (from non-Dpy F_1 mothers) were shifted to 25°C. *mat-1; mat-3* double mutants were then identified among the Dpy F_2 adults.

To construct the *mat-1(ax144ts);* HIS2B::GFP line, *unc-74(x19) mat-1(ax144ts)* heterozygous males were mated into AZ212*: unc-119(ed3); ruIs32 [pAZ132]* III. This strain contains an integrated histone (H2B) GFP transgene expressed under the *pie-1*

Table 1. *mat-1* temperature-allelic series

	15°C		20°C		25°C	
Allele	% hatch	mei/arm	% hatch	mei/arm	% hatch	mei/arm
Wild type	99.1±0.5	0.6±0.5	98.4±0.5	0.7±0.5	98.0±1.4	0.5±0.5
him-8	87.6±7.9	0.9±0.5	78.3±2.4	0.8±0.4	85.5±6.2	0.6±0.5
ax212ts; him-8	87.4±3.1	1.8±0.3	87.3±3.5	1.9±0.5	13.7±8.5*	1.1±0.2
ye121ts	100±0	0.9±0.3	99.3±0.5	1.1±0.6	0.0±0.0	100%
ye121ts; him-8	84.0±5.3	0.7±0.5	89.2±7.1	1.2±0.4	0.0±0.0	100%
ax161ts	58.4±17.0	2.4±0.6	16.3±12.5	3.2±1.0	0.0±0.0	100%
ax161ts; him-8	87.8±5.3	1.9±0.7	12.6±8.5	2.8±0.5	0.0±0.0	100%
ax227ts; him-8	89.3±2.7	2.2±0.6	12.5±7.7	3.1±0.7	0.0±0.0	100%
ax72	1.7±1.7	3.1±1.3	4.8±5.9	4.4±2.3	0.0±0.0	100%
ax144ts; him-8	47.2±11.1	1.5±0.5	0.0±0.0	100%	Sterile	NA
ax520	0.4±0.5	4.9±1.2	0.7±1.9	100%	Sterile	NA

Hermaphrodites of the indicated genotypes were either kept at 15°C or shifted from 15°C to the indicated temperature as L1 larvae. In all cases, mutant hermaphrodites were crossed with wild-type males to ensure that only maternal effects were being scored. % hatch represents the average ratio of hatching L1 larvae to dead embryos, determined from complete clutches of 4-8 hermaphrodites. The average number of meiotic embryos per uterine arm (mei/arm) was determined from Nomarski observations of 10-20 adult hermaphrodites. Color coding reflects in utero data. Blue – uterus contains embryos of all stages and most embryos hatch. Green – uterus contains both excess meiotic embryos and multicellular embryos. Red – uterus contains only meiotic one-cell embryos. Boxes – groups in which individual hermaphrodites were found to be of either color class.

*Data collected from the subset of animals that produced embryos.

promoter (Praitis et al., 2001). Unc-74 animals were examined in subsequent generations for GFP expression until a line segregating all GFP-positive animals was found. This *unc-74(x19) mat-1(ax144ts); ruIs32* line was used for the images in Fig. 1.

RNA-mediated interference (RNAi)

PCR primers containing T7 polymerase binding sites were used to amplify an ~850 bp fragment of the cDNA clone yk466b3, an EST clone corresponding to Y110A7A.17. This PCR fragment was used to synthesize dsRNA using the T7 Megascript Transcription kit (Ambion Inc., Austin, TX) according to manufacturer's instructions. dsRNA was injected into either wild-type animals (N2 strain) or animals containing the integrated histone H2B::GFP transgene (strain AZ212) (Praitis et al., 2001). After a 16- to 20-hour recovery period, gravid AZ212 mothers were directly examined for GFP expression in their embryos. In other experiments, gravid N2 or AZ212 mothers were dissected and their progeny were either examined directly for GFP expression or were fixed and stained for immunofluorescence according to previously published protocols (Golden et al., 2000). Similar results were observed when RNAi experiments were performed by standard feeding protocols (Fraser et al., 2000; Timmons et al., 2001) using a construct created by Wallenfang and Seydoux (Wallenfang and Seydoux, 2000). To observe hypomorphic *mat-1* phenotypes (Fig. 1F), L4 animals were fed at 15°C and progeny were examined 20-24 hours later. For *sep-1* RNAi feeding, the bacterial strain expressing *sep-1* dsRNA (Zipperlen et al., 2001) was used to feed the *C. elegans* strain AZ212 at 20°C and progeny were examined 12-16 hours later.

cDNA synthesis and DNA sequencing

The open reading frame of Y110A7A.17 was confirmed by sequencing the yk10h2 and yk466b3 cDNAs. To obtain the complete 5′ UTR sequence, cDNA was PCR-amplified from wild-type animals using an SL1 5′ primer and a primer within the coding sequence. DNA sequencing revealed a cDNA identical to the Y110A7A.17 coding region predicted by the *C. elegans* sequencing consortium (http://www.wormbase.org/). cDNA synthesis and DNA sequencing of Y110A7A.17 from the various *mat-1* alleles was performed essentially as described by Golden et al. (Golden et al., 2000). The GenBank accession number for the full-length cDNA is AY081955.

Immunohistochemistry and phenotypic analysis

For immunohistochemical analysis of embryos, germline and somatic tissue, adult animals were transferred to an 11.5 μl drop of egg buffer (Edgar, 1995) on a poly-l-lysine-subbed Color Frost Plus slide (Sigma-Aldrich, Fischer Scientific). Embryos and gonads were extruded using a 27.5 gauge needle, covered with a 24×50 mm SuperSlip coverslip (Fischer Scientific), freeze cracked and processed for antibody staining. For tubulin and phospho-histone H3 antibody staining, similar protocols and reagents were used as previously described (Golden et al., 2000).

The in utero defects of L1 upshifted animals were analyzed either with DIC optics or epifluorescence (for H2B::GFP transgenic animals) of living adult animals (Praitis et al., 2001; Sulston and Horvitz, 1977). The germline defects of L1 upshifted animals were analyzed by UV epifluorescence in whole mount, DAPI (4′,6′-diamidino-2-phenylindole)-stained animals that were fixed with Carnoy II fixative (6:3:1 ethanol/acetic acid/chloroform).

Growth conditions

Animals were grown on a lawn of *E. coli* (strain OP50) on MYOB plates (Church et al., 1995). The analysis of *mat-1* male phenotypes was carried out in the mutant background *him-8(e1489)*, a mutation that increases the frequency of males by specifically increasing non-disjunction of the X chromosomes (Hodgkin et al., 1979); but which does not significantly enhance the *mat-1* defects under restrictive conditions (Table 1). For the analysis of semi-synchronous L1 upshifted males and hermaphrodites, ten or more *mat-1; him-8* hermaphrodites of a given allele were allowed to lay embryos on MYOB agar plates for 8-12 hours at 16°C before being removed. As soon as 75% of these embryos had hatched, the plate of largely L1 larvae was shifted to 25°C, and the animals were subsequently analyzed 42 hours later as young adults. Alternatively, developmentally arrested L1 larvae were collected from freshly starved plates and transferred to 25°C plates with food. In late-stage upshift experiments, animals were semi-synchronized by selecting L4 larvae from mixed-stage, 15°C populations and shifting them to the indicated temperature either as L4 larvae or as young adults for a specified duration.

The upshifted *ax72* and *ax520* homozygotes reported in this analysis were collected from the progeny of balanced heterozygotes, since these homozygotes produce dead embryos even when raised at 15°C.

To ensure that our analysis of embryos was confined to the *mat-1* maternal effects and not its paternal effects (Golden et al., 2000; Sadler and Shakes, 2000), the *mat-1* hermaphrodites in these studies were mated to wild-type males. Importantly, with the exception of *ax520* and *ax144ts*, *mat-1* embryos exhibited similar defects regardless of whether their hermaphroditic parents had been upshifted before, during, or after the L4 larval period, when *C. elegans* hermaphrodites generate their full complement of sperm.

For L4 upshift studies, 10-20 young L4 stage animals that were reared at 15°C were picked onto a fresh plate and shifted to specific temperatures ranging from 20 to 25°C for specified time intervals. For analysis, animals were dissected, fixed and stained for immunohistochemistry. The 15°C and 20°C incubations were done in a Precision Scientific Low Temperature Incubator 815 (±0.3-0.5°C). The 24°C studies were done in an Echotherm (TM) Bench Top Chilling Incubator (±0.01°C). The 25°C studies were done in a Percival Scientific 30 Series Incubator (±0.2°C). The temperatures were monitored with a Barnant RTD (Platinum) Datalogger.

RESULTS

mat-1 encodes the *C. elegans* homolog of the APC/C subunit CDC-27/APC-3

As four other genes associated with Mat mutant phenotypes (Davis et al., 2002; Furuta et al., 2000; Golden et al., 2000) were subsequently shown to encode subunits of the APC/C, it seemed likely that *mat-1* also encoded an APC/C related gene. To test this, we searched the *C. elegans* sequence database for candidate genes within the genetic interval known to contain *mat-1* (Golden et al., 2000). Within this region is the single *C. elegans* homolog of *cdc-27/apc-3*. To determine whether this *cdc-27/apc-3* homolog (Y110A7A.17) would produce a metaphase I arrest phenotype, we performed RNAi with a corresponding EST clone (Fire et al., 1998; Hunter, 1999). While the uteri of wild-type control hermaphrodites were filled with rapidly dividing embryos of many different ages (Fig. 1E,I), the uteri of hermaphrodites that had been injected with double stranded *Ce-cdc-27* RNA were filled with one-cell embryos (Fig. 1G). These *cdc-27(RNAi)* embryos looked like those from *mat-1* mothers when examined either in utero (Fig. 1H) or as individual fixed specimens that had been processed for DAPI staining and tubulin immunofluorescence (Fig. 1B-D). The *mat-1* and *cdc-27(RNAi)* embryos accumulated in an arrested but otherwise normal metaphase I state (Fig. 1A). In all cases, the oocyte chromosomes were aligned in a pentagonal metaphase plate on a barrel-shaped meiotic spindle, and the sperm chromosomes remained highly condensed. Such embryos also lacked polar bodies (the discarded products of the meiotic divisions) and had incompletely hardened eggshells.

To confirm that *mat-1* encoded the *C. elegans cdc-27/apc-3* homolog, the Y110A7A.17 ORF from each of the seven *mat-1* mutant alleles was PCR-amplified and sequenced. The sequencing data revealed unique missense mutations in the *cdc-27* ORF for each *mat-1* mutant allele (Fig. 2), indicating that *mat-1* does indeed encode the *C. elegans cdc-27* homolog. The seven mutations are scattered throughout the coding sequence; five mutations alter highly conserved residues while those in *ax520* and *ye121* lie immediately adjacent to highly conserved regions. None of the mutations affect potential phosphorylation sites, but five occur within the

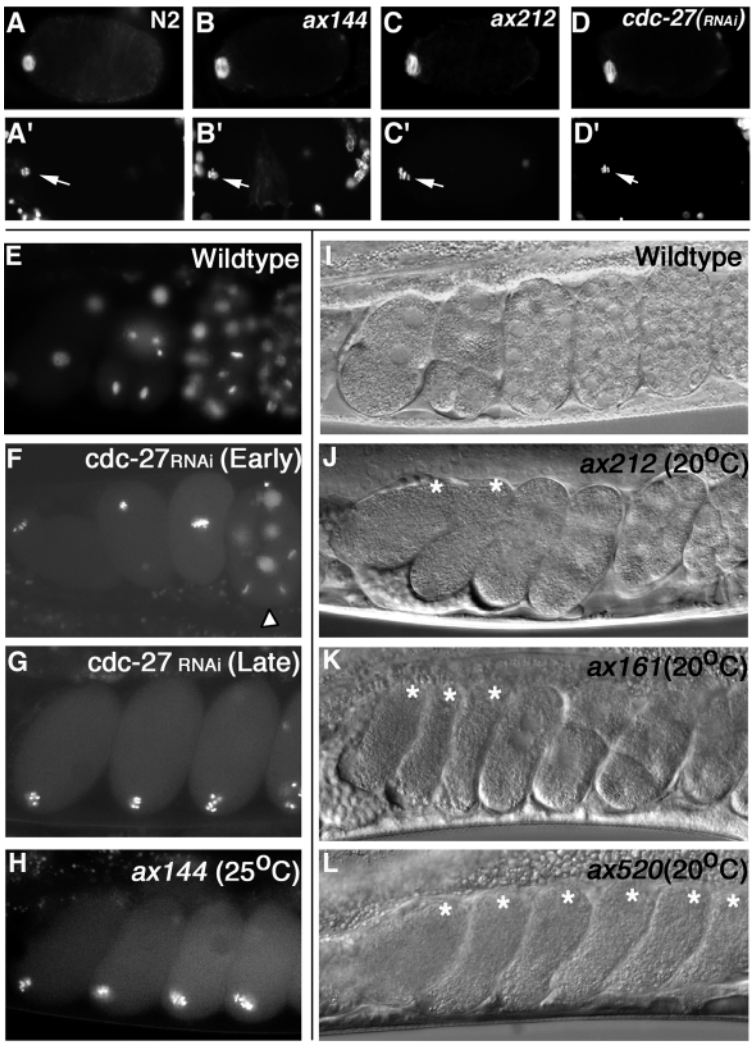

Fig. 1. Phenotypic analysis of *mat-1* mutant and *cdc-27* RNAi embryos. Micrographs show tubulin (A-D) and DAPI (A′-D′) staining of individual metaphase I embryos of wild type (N2) (A,A′), *mat-1(ax144)* at 25°C (B,B′), *mat-1(ax212)* at 25.5°C (C,C′) and *cdc-27* RNAi (late) (D,D′). White arrows indicates oocyte chromosomes. Only wild-type embryos progress to anaphase I and exit meiosis. (E-H) Micrographs of H2B::GFP embryos within the uteri of wild type (E), *cdc-27* RNAi (F,G) and *mat-1(ax144)* at 25°C (H). Non-viable multicellular embryos produced after 20-24 hours in *cdc-27* RNAi feeding experiments [(*cdc-27* RNAi (early); white arrowhead] and meiotic one-cell arrested embryos produced after 24 hours in RNAi feeding experiments [*cdc-27* RNAi (late)]. (I-L) DIC micrographs of embryos in the uteri of hermaphrodites incubated at 20°C. Wild type, *mat-1(ax212)* [permissive; 98.3% hatch], *mat-1(ax161)* [semi-permissive; 16.3% hatch] and *mat-1(ax520)* [restrictive; 0.7% hatch]. Meiotic one-cell embryos (asterisks) accumulate at all temperature regimes for all of the *mat-1* alleles (Table 1) but at permissive (J) and semi-permissive temperatures (K), the mutant embryos are able to exit meiosis and divide mitotically. At semi-permissive temperatures, the vast majority of the multicellular embryos (K) produced by *mat-1* hermaphrodites die prior to morphogenesis. The average embryo is ~50 μm in length.

conserved tetratricopeptide repeats (TPR) that are thought to mediate protein-protein interactions in a wide variety of proteins including three other APC/C components (Lamb et al., 1995).

Partial depletions of MAT-1 result in multicellular embryonic lethality

When adult hermaphrodites of any of the seven *mat-1* alleles were shifted to the restrictive temperature of 25.5°C for 12-24 hours as young adults, they produced metaphase I-arrested embryos that remained developmentally blocked in a meiotic one-cell state (Golden et al., 2000) (*ye121*, this study). This metaphase I-arrest phenotype is identical to the most extreme RNAi phenotype of any APC/C subunit (Davis et al., 2002; Furuta et al., 2000; Golden et al., 2000) and is likely to reflect the earliest function of the APC/C. However because this early block precludes the analysis of later functions, we reasoned that additional functions of the APC/C in either M-phase exit and/or early embryonic development could be studied in temperature-sensitive (ts) *mat-1* hermaphrodites raised at various intermediate temperatures. In these experiments, L1 larvae were shifted to various temperatures and their resulting clutches were scored for overall embryonic lethality and whether the affected embryos were dying as meiotic one-cell stage or multicellular embryos (Table 1). Multicellular embryonic lethality was previously reported in a subset of what are now known to be APC/C mutant alleles (Golden et al., 2000; Rappleye et al., 2002), but our finding that multicellular embryonic lethality is associated with all seven *mat-1* alleles at intermediate temperatures (Tables 1 and 2), confirms this as a general, rather than an allele-specific, phenotype. Similar phenotypes were observed when the levels of maternal *mat-1* mRNA were directly lowered by RNAi (Fig. 1F). When fed bacteria expressing *mat-1/cdc-27* dsRNA, affected wild-type hermaphrodites initially produced viable offspring, but subsequently produced a brief burst of multicellular dead embryos (20-24 hours) before producing only one-cell arrested embryos. These results, along with the observation of similar phenotypes in other temperature-sensitive APC/C mutants (Golden et al., 2000; Rappleye et al., 2002), suggest that this phenotype is associated with intermediate levels of APC/C activity rather than the specific disruption of either MAT-1 or a particular MAT-1 subdomain.

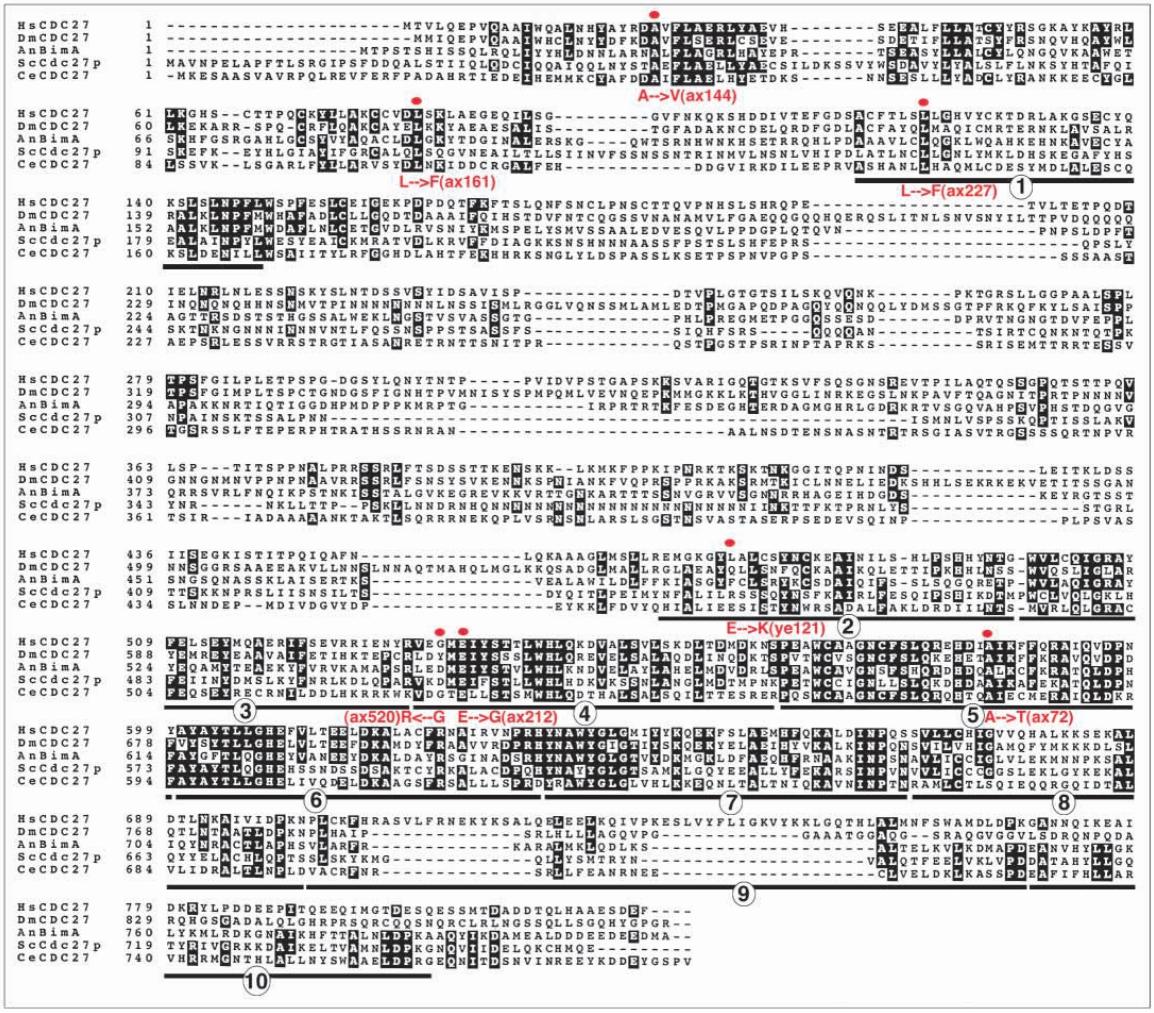

Fig. 2. Sequence alignment of *C. elegans mat-1/cdc-27* and its homologs from humans, *Drosophila*, *A. nidulans* and *S. cerevisae*. Identical residues are highlighted in black, conservative changes in gray, and the mutant lesions are indicated in red. Tetratricopeptide repeat (TPR) domains are underlined and numbered. Hs, *H. sapiens*; Dm, *Drosophila melanogaster*; An, *A. nidulans*; Sc, *S. cerevisiae* and Ce, *C. elegans*. Numbers on left represent amino acid positions.

Partial depletions of MAT-1 are associated with an extended meiosis I

Since *C. elegans* embryos presumably require the APC/C for both their meiotic and mitotic divisions, it was not obvious whether multicellular embryonic lethality, like the loss-of-function phenotype, would be specifically associated with defects in meiosis I or, alternatively with later defects in meiosis II or mitosis. To determine whether intermediate levels of APC/C activity were affecting a particular stage of early development, we scored the pattern of embryos within the uteri of *mat-1* hermaphrodites raised at various temperatures (see Materials and Methods). Because *C. elegans* oocytes are ovulated sequentially, the bilobed gonad of wild-type hermaphrodites produces a linear array of temporally ordered embryos within each half uterus. In wild-type hermaphrodites (and *ye121* hermaphrodites at 15°C), each half uterus typically contained 0-1 meiotic stage embryos followed by a single one-cell mitotic embryo and a series of progressively older multicellular embryos (Fig. 1I; Table 1). In contrast, the uteri of *mat-1* hermaphrodites contain a striking increase in the number of meiotic embryos. At permissive temperatures, *mat-1* hermaphrodites produced primarily viable embryos and contained 1-2 (±1) meiotic embryos per half uterus (blue in Table 1). Since new oocytes are ovulated every 20 minutes (McCarter et al., 1999), this result suggested that normal embryonic development can tolerate minor (20-40 minute) delays in meiotic progression. Under semi-permissive conditions, *mat-1* hermaphrodites accumulated 3-6 times as many meiotic embryos as same-temperature controls (green in Table 1; Fig. 1J,K) and, under fully restrictive conditions, *mat-1* hermaphrodites produced only meiotically arrested one-cell embryos (MeOC; red in Table 1; Fig. 1L). Ovulation rates were unaffected and could not account for the observed accumulation of meiotic embryos (data not shown).

To test whether these meiotic embryos were accumulating specifically in meiosis I or, alternatively, at various stages throughout meiosis, control and mutant embryos were dissected from wild-type or mutant mothers and prepared for DNA (DAPI) staining and anti-tubulin immunofluorescence. Embryos isolated from the uteri of wild-type mothers contained approximately equal numbers of meiosis I (MI) and meiosis II (MII) embryos indicating that these stages are normally of equal duration (Table 2). Under permissive conditions, *mat-1* hermaphrodites contained more meiotic embryos than wild-type controls (blue in Table 1), but roughly equal numbers of MI and MII embryos (Table 2). However, increasingly restrictive temperatures were associated with an increasing skew in the MI:MII ratios (green in Tables 1 and 2), and, at fully restrictive temperatures, only MI arrested embryos were observed.

Although semi-permissive temperatures were associated with significant mother to mother phenotypic variability (Table 1 and 2), inspection of the overall MI:MII ratios and polar body numbers revealed two phenotypic subgroups amongst multiple *mat-1* alleles. Less affected mothers produced MI, MII, and multicellular embryos, but owing to an extended MI, the MI:MII ratio was 3:1. Older embryos within such mothers had two positionally distinct polar bodies (2PB), indicating that both meiotic divisions had occurred. More severely affected mothers produced only MI and multicellular embryos. Whether examined by DAPI staining or DIC optics, these older embryos had only a single polar body (1PB), suggesting that they had exited meiosis after completing only a single meiotic division. Likewise, pronuclear stage embryos lacked the extra maternal pronucleus that would be expected if a second meiotic division had occurred in the absence of cytokinesis. Under conditions favoring the production of 1PB embryos, a few mothers within the population produce MII embryos, resulting in an overall MI:MII ratio of 9:1 (Table 2), however such variation was not observed amongst sibling embryos from the same mother. For clarity, we will hereafter refer to individual embryos as belonging to the ‘1PB class’ or ‘2PB class’.

Table 2. Meiosis I embryo accumulation in *mat-1* hermaphrodites

Genotype	Temperature (°C)	MI/MII	%MI	In utero embryo phenotype
N2	20º	11/9	55%	MC
him-8	20º	13/8	62%	MC
ax212	20º	14/9	61%	MC
ax212	23º	13/6	68%	MC
ax212	24º	24/7	77%	MC
ax212	25º	20/2	91%	MC (1PB)
ye121	20º	23/14	62%	MC
ye121	23º	45/16	74%	MC
ye121	24º*	50/5	91%	MC (1PB)
ye121	24º	35/0	100%	MEOC
ye121	25º	68/0	100%	MEOC
ax161; him-8	16º	18/11	62%	MC
ax161; him-8	20°	24/7	77%	MC
ax161; him-8	23º	27/0	100%	MEOC
ax161; him-8	24º	20/0	100%	MEOC
ax161; him-8	25º	25/0	100%	MEOC
ax227	20º	51/6	89%	MC (1PB)
ax227	23º	50/0	100%	MEOC†
ax72	16º	34/4	89%	MC (1PB)

Hermaphrodites (10-20) of the indicated genotypes were kept at 15ºC or shifted from 15ºC to the indicated temperature as young L4 larvae. Unless otherwise noted, the duration of incubation was 16-20 hours prior to analysis. In all cases, mutant hermaphrodites were crossed with wildtype males to ensure that only maternal effects were scored. The embryos were fixed and stained with DAPI and α-tubulin antibodies for staging. % MI represents the number of meiosis I embryos produced divided by the total number of meiotic embryos scored. The in utero phenotype column reflects the oldest and most predominant embryonic stage produced by the treated hermaphrodites. (MC, multicellular embryos; MEOC, meiotic one-cell embryos.)

The 1PB after MC indicates that the majority of treated hermaphrodites (>50%) produced embryos containing a single polar body. MC alone implies that the 2PB Class predominates.

*Hermaphrodites were incubated 12 hours prior to analysis.

†*ax227* at 23-25ºC produces 100% MEOC.

Blue-permissive condition (>85% hatch), Green – semi-permissive condition (2-20% hatch).

Red – restrictive condition (0% hatch).

Multicellular embryonic lethality is associated with severe meiotic defects

In contrast to previous reports (Rappleye et al., 2002), hypomorphic *mat-1* embryos proved to exhibit striking meiotic defects. In wild-type *C. elegans* embryos, there are four basic stages to each meiotic division (Fig. 3A-D). In mature MI oocytes, nuclear envelope breakdown occurs just prior to fertilization. Fertilization is followed by the rapid assembly of an anastral meiotic spindle and the congression and alignment of paired oocyte homologs on a metaphase plate (Fig. 3A).

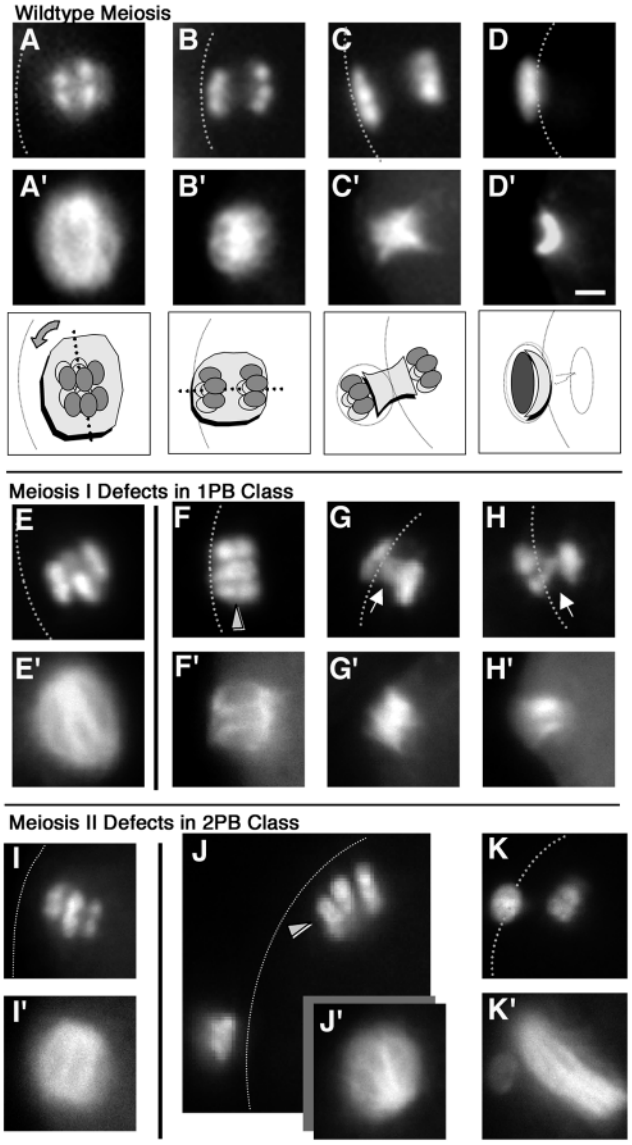

Fig. 3. Reductions in APC/C activity result in meiotic defects. DAPI (A-K) and tubulin (A′-K′) localization of meiotic chromosomes and spindles in wild type (A-D) and mutant *mat-1* (E-K) embryos. The dotted white lines represent the approximate position of the plasma membrane. After fertilization, oocytes progress through MI metaphase (A,A′), anaphase A (B,B′), anaphase B (C,C′) and telophase (D,D′; only chromosomes within the polar body can be seen in this focal plane). During oocyte meiosis, the metaphase to anaphase transition promotes a 90° rotation of the anastral spindle axis (A,B,A′,B′; see cartoon below. The dotted black line represents the long axis of the spindle). Consequently, one pole of the spindle abuts the plasma membrane (B′; see cartoon below). The cartoon series shows the organization of the meiotic chromosomes and spindles during wild-type meiosis. (E-K′) *mat-1* mutants incubated at restrictive and semi-permissive temperatures have meiotic defects. (E,E′) A metaphase plate and spindle from a metaphase arrested *mat-1(ax212)* embryo. (F′) Spindle rotation without chromosome separation (F; gray arrowhead) from a *mat-1(ax72)* embryo at 16°C. (G,H) Examples of MI anaphase bridges (white arrows) in *mat-1(ax227)* at 20°C (G) and *mat-1(ax72)* at 16°C (H). (I,I′) In the small percentage of the embryos that hatch at semi-permissive temperatures, normal meiosis I and II figures are seen [i.e., metaphase II (I,I′; the first polar body is outside of the field)]. (J,J′) Despite spindle rotation (J′), chromosome separation during meiosis II is not always normal (gray arrowhead). (K,K′) An example of an abnormal elongated meiotic spindle and an abnormally small array of meiosis II chromosomes [*mat-1(ax161)*]. Scale bar: (in D′) 2 μm.

During early anaphase I (Fig. 3B) the homologs separate as the spindle shortens and then rotates to a position perpendicular to the cortex (Albertson, 1984). By late anaphase I (Fig. 3C), a prominent microtubule bundle lies almost entirely between the separated homologs and possesses a morphology reminiscent of a cinched haystack. During telophase I (Fig. 3D) the individual chromosomes coalesce into two opposing chromatin masses as the spindle splits during the highly asymmetric cell division that forms the first polar body. This sequence is reiterated during MII but is immediately followed by nuclear envelope formation and a round of DNA synthesis. In the absence of a functional APC/C, embryos remained blocked in metaphase I; with time, the meiotic spindle disassembles but nuclear envelopes never reassemble (Golden et al., 2000).

As in the fully restrictive meiotic arrest class, *mat-1* embryos of the 1PB class assembled their paired homologs into a normal metaphase I spindle (37/37; Fig. 3E). However, the subsequent steps of spindle rotation and polar body formation occurred in the absence of homolog separation (Fig. 3F′). As a result, anaphase and telophase-like spindles had prominent chromosome bridges between the two DNA masses (Fig. 3G,H). Such polar bodies were stable but frequently contained misshapen and fragmented DNA, suggesting that the process of polar body formation ‘cuts’ these DNA bridges in half, as happens during the mitotic divisions of hypomorphic *S. pombe* APC/C mutants (Funabiki et al., 1996a). Consistent with meiotic chromosome segregation defects, the maternal pronuclei of early post-meiotic embryos also were frequently misshapen (data not shown). Similar defects were observed in both meiotic divisions of 2PB class embryos. Analysis of MII embryos revealed relatively normal metaphase figures (Fig. 3I,I′), yet MII spindle rotation and second polar body formation occurred in the absence of sister chromatid separation (Fig. 3J), resulting in a MII ‘cut’ phenotype. In addition, mutant spindles were frequently longer than wild type (Fig. 3K′). These MII defects suggest a role for the *C. elegans* APC/C in either spindle shortening or MII, although our data do not preclude the possibility that many or all of these MII defects are a secondary consequence of MI abnormalities. Importantly, we identified no semi-permissive temperature conditions that resulted in either metaphase II arrest or an accumulation of MII embryos.

Specific meiotic defects correlate with specific developmental consequences

In wild-type *C. elegans* embryos, there is a predictable and tight correlation between the developmental and cell cycle events of the one-cell stage (Sadler and Shakes, 2000). Key developmental events include the formation of an impermeable, three layer eggshell during the late meiotic phase (Chitwood and Chitwood, 1974) and the post-meiotic establishment of the embryo’s anterior-posterior (AP) axis (for reviews, see Gotta and Ahringer, 2001; Lyczak et al., 2002;

Table 3. Hypomorphic *mat-1* mutants divide symmetrically during the first mitotic cell division

			Larger blastomere/embryo size (% embryos)						
	n	Temp.	50-51	52-53	54-55	56-57	58-59	60-61	62-63
N2	21	20° const.	0	0	5	19	**62**	14	0
ax161	14	YA to 20°	0	0	14	**43**	**29**	14	0
ax161	6	L4 to 20°	**33**	0	17	17	0	**33**	0
ax72	18	15° const.	22	22	22	11	11	0	11
ye121	22	YA to 23°	0	5	14	**59**	18	0	5
ye121	21	L4 to 23°	10	14	10	**29**	14	10	5
ye121	16	YA to 24°	**25**	19	13	0	**31**	13	0
ye121	17	L4 to 24°	**47**	**30**	6	12	0	6	0

Mutant animals of the indicated genotype were raised at 15°C and shifted to the indicated temperature as either young adults (YA) or L4 larvae on plates with wild-type males. After 14-18 hours, two-cell embryos were isolated from mutant mothers and imaged under Nomarski optics. Blastomere areas were calculated from perimeter tracings using IPLab software. In table, percentages ≥25% are in bold.

Pellettieri and Seydoux, 2002). Importantly, AP polarization appears to be triggered, in part, by growth of the sperm-derived microtubule asters (O'Connell et al., 2000; Sadler and Shakes, 2000; Wallenfang and Seydoux, 2000). AP polarization culminates in a highly asymmetric first mitotic cell division that results in the formation of sister blastomeres that differ in size, synchrony, and the orientation of their cell divisions.

Metaphase I arrested *mat-1/cdc-27* (*RNAi*) embryos fail to develop either an impermeable eggshell or a stable A-P axis, indicating that the early cell cycle block is coupled with a corresponding developmental block (Golden et al., 2000; Wallenfang and Seydoux, 2000) (this study). To determine the effect of a partial APC/C depletion, embryos from *mat-1* mothers grown under semi-permissive conditions were analyzed for eggshell and polarization defects. Mutant embryos with two distinct polar bodies made eggshells that were impermeable to the lipid soluble DNA dye Hoechst 33248 whereas mutant embryos with a single polar body made Hoechst-permeable eggshells. To assess potential polarization defects, dividing sister blastomeres of either mutant or wild-type two-cell embryos were scored for their relative size, synchrony and spindle orientations (Table 3, Fig. 4). Compared to wild-type controls, hypomorphic *mat-1* embryos either exhibited increased variability in the positioning of their first cleavage plane (Table 3) or, under increasingly stringent conditions, divided symmetrically. Symmetric divisions were strongly correlated with the presence of a single polar body (14/14; Fig. 4N,O). In general, sister blastomeres of such 1PB class embryos divided synchronously with both spindles oriented perpendicular to the long axis of the embryo (Fig. 4N,O). In contrast, those of 2PB class embryos were variably intermediate in their relative size, synchrony, and cleavage orientations (15/15; Fig. 4I,J). Lastly, although germline-specific P-granules segregated normally in most 2PB class embryos, P-granule segregation failed in both MI-arrested embryos and in symmetrically and synchronously dividing 1PB class embryos (data not shown). In summary, 1PB class embryos exhibited consistently more severe defects in the symmetry, timing, and cleavage orientations of their early cell divisions when compared with either 2PB class embryos or wild-type controls.

1PB class embryos exhibit defects during meiotic exit and the pronuclear one-cell stage

To determine whether the defects observed in dividing two-cell embryos were being presaged by abnormalities during the earlier pronuclear stage, we compared pronuclear-stage mutant embryos with same-stage control embryos using either DAPI/tubulin staining or DIC microscopy. During the pronuclear stage of wild-type embryos, the replicated sperm centrosomes expand and separate to lie on opposite sides of the male pronucleus, and the female and male pronuclei migrate to join in the posterior half of the embryo (see Fig. 4A-C for an early migration stage). In 12/12 2PB class *mat-1* embryos (Fig. 4F-H), sperm aster maturation and pronuclear migration remained unaffected. In contrast, 1PB class *mat-1* embryos exhibited numerous defects (Fig. 4K-M). In wild-type embryos, increased cytoplasmic flow rates immediately prior to the initiation of pronuclear migration promote the rapid relocation of the male pronucleus to the presumptive posterior end (Fig. 4A) (see also Goldstein and Hird, 1996). Such flows were absent in 1PB mutant embryos, and in 15/15 same-stage embryos, the male pronuclei failed to relocate from their initial cortical position to one of the two embryonic ends (Fig. 4K). In addition, both the expansion and separation of the sperm asters was delayed (Fig. 4L,M).

Displaced male pronuclei have also been reported in embryos partially depleted of separase, the key effector of metaphase APC/C activity (Rappleye et al., 2002). Our own observations revealed that wild-type mothers fed for a specific short time on *sep-1* dsRNA-producing bacteria produce embryos that specifically fail to relocate their male pronuclei. However, in striking contrast to the earlier report, such defects were always associated with severe meiotic defects, namely the presence of a single polar body (12/12; Fig. 5).

To determine if the pronuclear and cleavage defects in 1PB class *mat-1* embryos could be a secondary consequence of even earlier meiotic exit defects, we compared the process of meiotic exit in wild-type and 1PB class embryos. In mitotic cells of other organisms, the APC/C is known to drive M-phase exit by poly-ubiquitinating B-type cyclins and activating the mitotic exit network (McCollum and Gould, 2001). In one-cell *C. elegans* embryos, exit out of MII is complex because it involves both a direct M to S transition (no apparent G1) and the final conversion of the fertilized oocyte into a zygote. This M to S phase transition is marked by several events including the disappearance of M-phase cell-cycle markers such as phosphorylated histone H3 (p-H3) (Fig. 6), the extensive remodeling of the sperm chromatin, the disassembly of the meiotic spindle, and the duplication and nucleation of the paternally derived centrosomes (Albertson and Thomson, 1993; Sadler and Shakes, 2000).

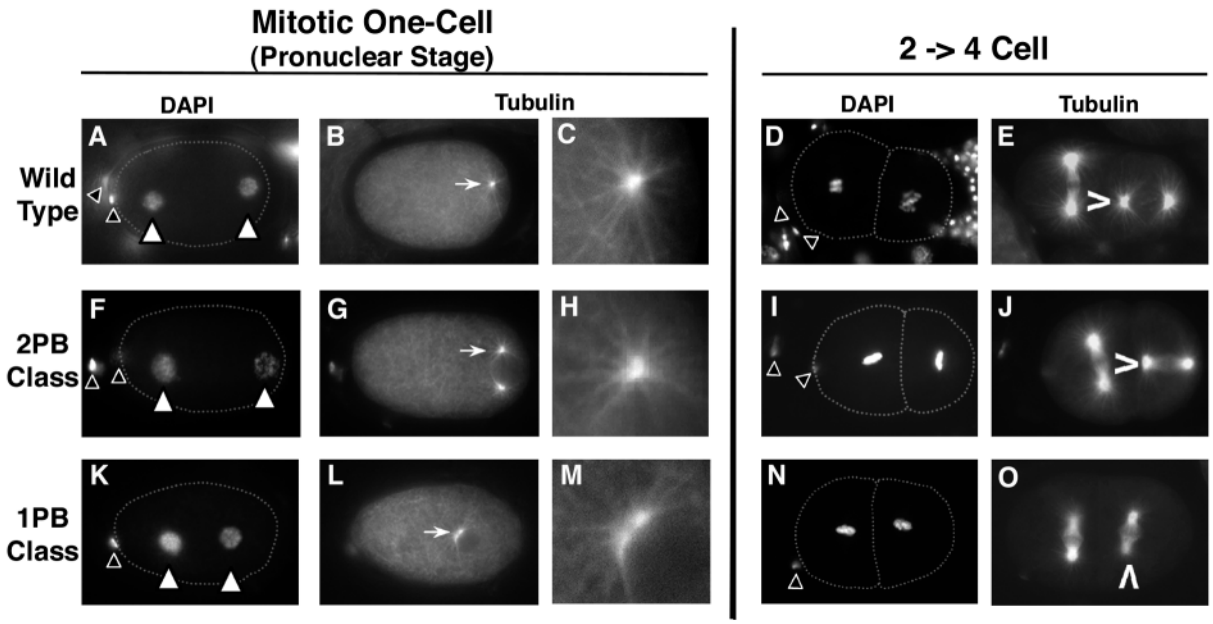

Fig. 4. Developmental consequences of the reduction in APC/C activity in the early embryo. DAPI and tubulin localization during the pronuclear stage and two- to four-cell stage in wild-type embryos (A-E) and *mat-1* 2PB class (F-J) and 1PB class embryos (K-O). (A-C) Wild-type pronuclear stage embryo in which the sperm pronucleus (A; right white arrowhead) is anchored in the peripheral cortex by the sperm asters (B, white arrow). The female pronucleus (A; left white arowhead) is positioned more centrally. The centrosomes of the sperm aster lie on opposite sides of the sperm pronucleus (B, other centrosome is below the focal plane) and each centrosome has multiple microtubules emanating from the centrosome to the cortex (C). (D) Dividing wild-type two-cell embryos have two polar bodies (black arrowheads; one polar body is outside the focal plane), a larger blastomere (left) and a smaller blastomere (right). The second mitotic division is asynchronous and the individual spindles set up perpendicular to each other (E). (F-J) In the less severely affected 2PB class embryos (F,I; black arrowheads indicate position of the two polar bodies), the relative position of the female pronucleus is normal (F; left white arrowhead). In addition, the sperm asters and microtubules extend normally from each centrosome to the cortex (G,H). (I,J) Although the relative blastomere size and cleavage orientation of the two blastomeres are similar to wild type, the mutant blastomeres tend to divide more synchronously. (K-O) Under semi-permissive temperature conditions when MI predominates (K,N; black arrowhead indicates single polar body), embryos exit meiosis but zygotic development is severely compromised. The pronuclear stage of this 1PB class is characterized by abnormalities in the relative positions of the pronuclei (K) and the maturation of the sperm asters (L,M). The first division in this 1PB class is symmetric (N). In the second division, the blastomeres divide synchronously with both spindles perpendicular to the long axis of the embryo (N,O). C, H and M are enlargements (4×) of the sperm asters in B, G and L. The carets in E, J and O indicate the orientation of the mitotic spindle of the right blastomere of two- to four-cell embryos. The average embryo is ~50 μm in length.

In wild-type embryos, late anaphase II can be distinguished from post-meiotic S phase on the basis of DAPI/tubulin/p-H3 staining patterns (Fig. 6). During late anaphase II, the highly condensed, maternally derived sister chromatids stain brightly with anti-p-H3 (Fig. 6C,E). In contrast, the highly condensed, paternally derived chromatin mass fails to stain with anti-p-H3, and its associated centrosome remains quiescent (Fig. 6B,D,F). During M-phase exit, each chromatin set decondenses and becomes enclosed within a pronuclear envelope (Fig. 6I,J). At the same time, p-H3 staining is rapidly lost from the female pronucleus while the chromatin within the second polar body continues to stain brightly (Fig. 6K). Also at this stage, the newly formed second polar body is associated with a compact, flattened spindle remnant at the cortical surface (Fig. 6G), while the sperm centrosome duplicates and begins to nucleate microtubules (Fig. 6H).

Analysis of M-phase exit in 1PB class embryos revealed several striking abnormalities. In particular, the post-meiotic maternal chromosomes continued to stain with p-H3 antibodies, albeit unevenly, even after nuclear envelope reformation (10/10; Fig. 6Q). In addition, the male pronucleus sometimes stained aberrantly with p-H3 (5/10; Fig. 6R) even after centrosome duplication and the initiation of aster formation (Fig. 6N). In addition, such embryos frequently contained large, disorganized meiotic spindle remnants that, unlike their wild-type counterparts, appeared to extend into the cortical interior (Fig. 6M). Such defects suggest that the aberrant meiotic exit of the 1PB class directly out of MI disrupts the normal coordination of the various cellular events that accompany the process of meiotic exit and that set the stage for the proper development of the zygote.

Analysis of APC/C double mutants reveal latent mitotic defects in apparently meiotic-specific alleles

In previous studies, a subset of temperature-sensitive *mat* alleles were found to exhibit defects not only in the meiotic divisions of the post-fertilization embryo but also in the mitotically proliferating germline, male tail and hermaphrodite vulva (Furuta et al., 2000; Golden et al., 2000). Amongst *mat-1* alleles, only two alleles (*ax144* and *ax520)* proved to result in significant germline proliferation defects (Golden et al., 2000) (Table 4; Fig. 7) and only three alleles (*ax144*, *ax520* and *ax212*) produced significant defects in the male tail and hermaphrodite vulva (Table 4; Fig. 8). In contrast, other alleles

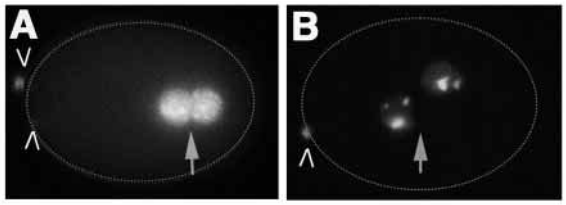

Fig. 5. *sep-1* RNAi mimics the 1PB APC/C phenotype. (A,B) H2B::GFP micrographs of individual post-meiotic one-cell stage zygotes. The wild-type zygote in A has completed both meiotic divisions (carets point to the two polar bodies, one is out of the focal plane) and is at the pronuclear migration stage of zygotic development. The female pronucleus (left) travels from the far left end of the zygote to meet up with the male pronucleus (right). Pronuclear meeting normally occurs within the right end of the embryo (arrow). The *sep-1* RNAi zygote in B has completed only a single meiotic division prior to developing pronuclei (arrowheads point to the single polar body). Like the APC/C 1PB class, SEP-1 depleted zygotes remain in a meiosis I stage and fail to progress to meiosis II. The *sep-1* RNAi zygote transitions directly into an abnormal pronuclear stage embryo (cortical contractions and flows are absent). As in the 1PB class, the female pronucleus and the male pronucleus meet centrally within the cell (arrow). The chromosomes in both pronuclei appear more condensed than in wild-type zygotes.

either resulted in no mitotic defects or moderate defects in only a subset of the population (Table 4). Although such results could suggest that the other *mat-1* alleles were meiotic specific, the discovery that the *mat-1* molecular lesions were scattered throughout the protein (Fig. 2) suggested that the meiotic divisions of the oocyte may simply be more sensitive to a partial loss of APC/C function. If the apparent allele-specificity was merely a matter of dosage, additional *mat-1* alleles might be expected to display mitotic defects in double mutant combinations with other APC/C genes.

To test whether mutations in other APC/C subunits could enhance the phenotype of the relatively unaffected alleles and thus uncover 'latent' APC/C mitotic defects, we selected *ax212* and *ax227* as appropriate Mel (maternal-effect lethal) alleles. At 15°C *ax212* and *ax227* hermaphrodites are fully fertile, and at 25.5°C they produce clutches of meiotic one-cell embryos but do not exhibit the sterility (ste) associated with significant germline and somatic defects. In these studies, we constructed doubles of *mat-1(ax212)* and *mat-1(ax227)* with alleles of *mat-2/apc-1*, *mat-3/cdc-23*, *emb-27/cdc-16* and *emb-30/apc-4* that are known to be Mel but not sterile in L1 upshift experiments (Golden et al., 2000). At 15°C, all of the double mutants developed to adulthood, but some of these double mutant mothers produced clutches of

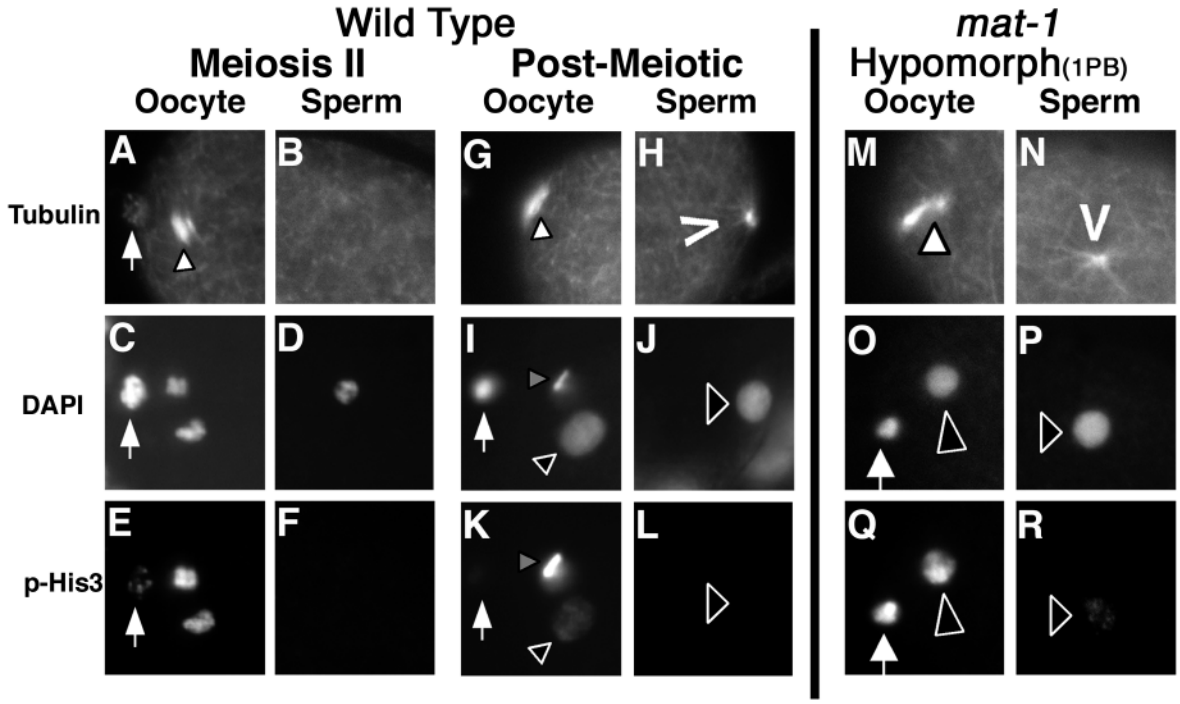

Fig. 6. Meiotic exit is compromised in embryos with reduced APC/C activity. Localization of tubulin, DAPI and phospho-histone H3 (p-H3) in wild type (A-L) and *mat-1* meiotic hypomorphs (M-R). Wild-type telophase II is characterized by the presence of a single polar body (white arrow in A,C,E,I) and a MII spindle (A; white arrowhead) that lies between two p-H3 staining (E) haploid chromosome sets (C). In early post-meiotic embryos, the compact MII spindle remnant lies at the surface of the plasma membrane (G; white arrowhead). Both the first (I, white arrow) and second (I, gray arrowhead) polar bodies can be seen, but only the second stains with p-H3 (K). At this stage, both the female (I, black arrowhead) and male pronucleus (J) have formed. The female, but not the male, pronucleus stains weakly with p-H3 (K,L). *mat-1* hypomorphs (1PB class) display variable meiotic exit defects, with post-meiotic mutant embryos retaining many meiotic characteristics. Typical defects include large, disorganized meiotic spindle remnants (M; white arrowhead) co-existing with the developing sperm aster (N; caret). When the pronuclei form, only a single polar body (O; white arrow) is present and both the female pronucleus (O; black arrowhead) and polar body stain brightly with p-H3 (Q). In some 1PB class embryos, the male pronucleus (P; black arrowhead) was found to abnormally stain for p-H3 (R; black arrowhead).

Table 4. Mitotic defects

	Wild type	ye121	ax161	ax227	ax72	ax212	ax144	ax520
In utero embryos	Hatch	MEOC	MEOC	MEOC	MEOC*	MC*	None	None
Germ line prolif.	100%	100%	97% 0% 3%	100%	65% 35%	82% 2% 16%	9% 7% 84%	4% 7% 89%
Herm. vulva	100%	100%	100%	100%	100%	87% 13%	48% 52%	31% 69%
Male tail	100%	87% 13%	98% 2%	100%	100%	49% 46% 6%	5% 44% 51%	0% 10% 90%

Animals were shifted from 15°C to 25°C as L1 larvae. Hermaphrodite gonads and hence germline proliferation were scored as normal (blue) if the distal tips had reflexed and extended beyond the spermatheca; many of the mutant gonads within this category were smaller than the wildtype controls. Gonads were scored as intermediate (green) if the gonadal arms extend and reflex but the distal tip do not extend beyond the spermatheca and severely affected (red) if they were either amorphous masses or small and linear. For gonad size measurements *n*=16-90. The in utero embryos from these hermaphrodites were scored as in Table 2 (MEOC, meiotic one-cell embryos; MC, multicellular embryo). Hermaphrodite vulvas were scored as wild type (blue) or everted (red); *n*=34-97. Male tails were scored as wild type (blue); as having some missing or fused rays (green); or possessing no or only a few rays (red). Males with severely affected tails frequently had abnormal spicules. For male tails, *n*=20-61.

*Embryos were present only within animals with full-sized gonads.

dead embryos (Table 5) suggesting that, even at 15°C, APC/C activity in *mat-1(ax227)* and *mat-1(ax212)* animals is not completely normal. To specifically test whether these double mutant combinations would exhibit 'latent' germline defects, *ax227* double mutants from heterozygous parents were shifted to the restrictive temperature as embryos or L1 larvae. While all of the double mutants developed through the adult stage, many were sterile (Table 5). Likewise, *mat-1(ye121); mat-3(or180)* doubles were also sterile at 25°C. Taken together, these results indicate that the molecular lesions in *ax212*, *ax227* and *ye121* are not meiotic-specific, even though, as single mutants, these alleles provide sufficient APC/C function to support normal germline proliferation. Although we did not observe enhancement of male tail and hermaphrodite vulva defects in these *mat-1* double mutant experiments, these somatic mitotic defects were enhanced in the double APC/C Mel combination of *emb-27(g48)* and *emb-30(g53)* (P.S., unpublished).

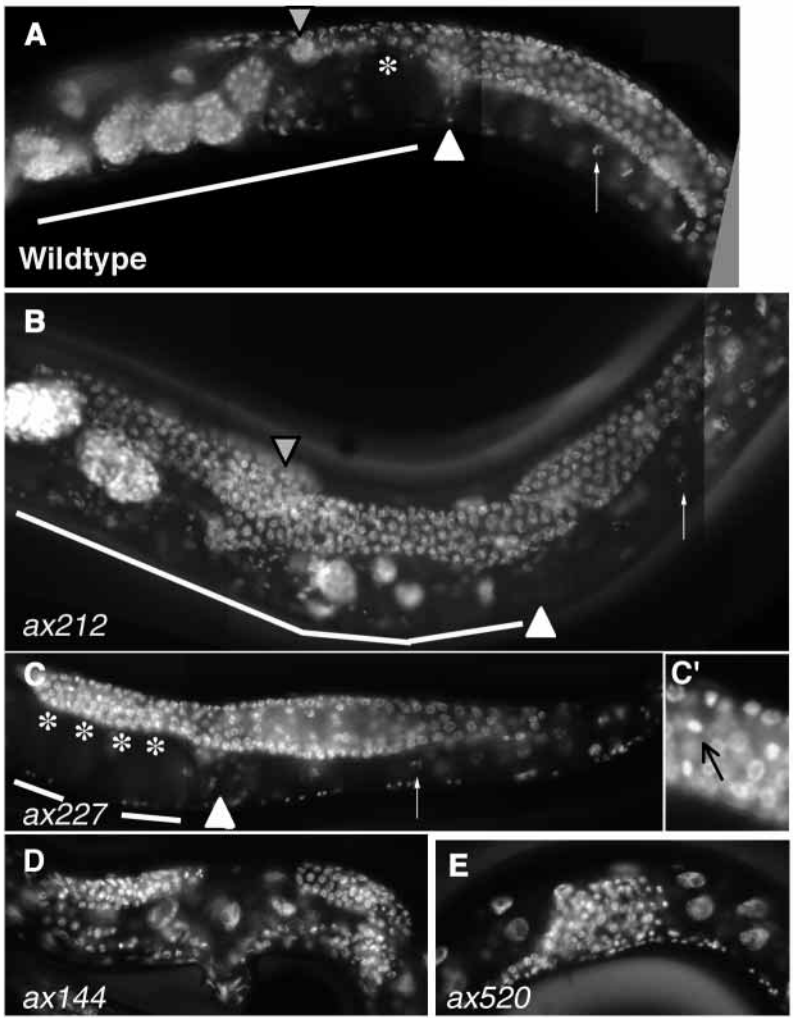

Fig. 7. Germline defects in *mat-1* hermaphrodites. Animals were shifted from 15°C to 25°C as L1 larvae and prepared for whole-mount DAPI staining as young adults. Images show one arm of a bilobed gonad (A,C), one arm plus the entire uterus (B), or the entire gonad (D,E). Oocytes can be identified by their diakinetic chromosomes (white arrows). In wild-type hermaphrodites (A), the gonad extends and reflexes so that the distal tips lie dorsally (gray arrowhead; distal tip is out of the plane of focus) over the vulva. Wild-type sperm with their highly condensed, haploid nuclei can be seen in the upper regions of the spermatheca (white arrowhead). Left of the spermatheca, a meiotic one-cell embryo (asterisk) and progressively older embryos lie within the uterus (white line). (B) A non-sterile, *ax212* hermaphrodite in which the distal tips overlap (gray arrowhead). The mutant sperm lack DNA (spermatheca; white arrowhead), and the uterus (white line) contains a mixture of viable and dead embryos. (C) In *ax227* hermaphrodites, the gonad is only slightly shorter than wild type but excess metaphase nuclei can be seen in the distal region of the gonad (C′; black arrow). The uterus contains only meiotic one-cell embryos (C; asterisks). In *ax144* and *ax520*, the gonad is significantly reduced (D) and amorphous (E) germlines lack both oocytes and sperm.

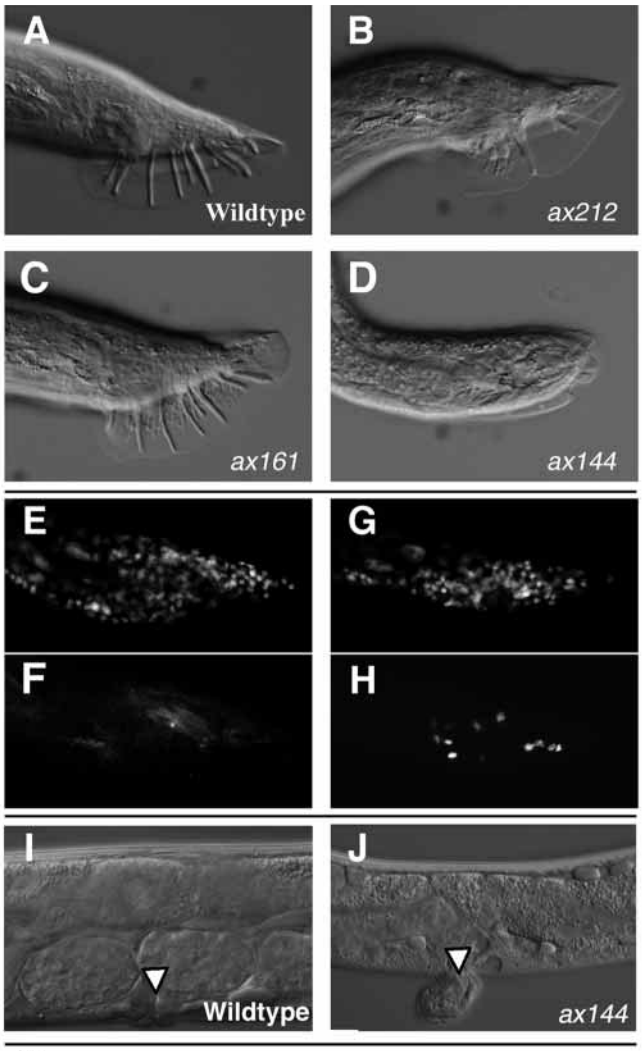

K. p-H3 staining of somatic nuclei in L4 male posterior

Allele	n	0	1-4	5-8	9-12	13-16
him-8	30	93%	3%	3%	0%	0%
ax144	33	0%	12%	42%	39%	6%

Fig. 8. Somatic defects in *mat-1* mutants. DIC images of tails from wild-type (A) or *mat-1* (B-D) young adult males that had been shifted from 15°C to 25°C as L1 larvae. *ax161* tails (C) are essentially normal, *ax212* tails (B) exhibit moderate defects including missing or fused rays, and the severely reduced *ax144* tails (D) typically lack rays altogether. Posterior regions of wild-type (E,F) and *ax144* (G,H) males that were shifted to 25°C as L1 larvae and processed for immunofluorescence as L4 larvae for DAPI (E,G) and p-H3 (F,H). In comparison to the wild-type controls (E,F), *ax144* animals exhibit reduced cell proliferation as assessed by DAPI-staining (G) and increased numbers of M-phase nuclei as assessed by anti-p-H3 immunofluorescence (H). (I) Wild-type vulva (white arrowhead). (J) Everted vulva (white arrowhead). (K) Quantitation of excess p-H3-staining somatic nuclei within the posterior of *mat-1* L4 males (30-36 hours after the L1 upshift).

APC/C related male tail defects are associated with M-phase delays

In previous studies, defects in the mitotic proliferation of germline stem cells were associated with mitotic metaphase I blocks and/or M-phase delays (Furuta et al., 2000; Golden et al., 2000) as were everted vulva (Evl) defects in *emb-30/apc-4* mutants (Furuta et al., 2000). For *mat-1* Evl phenotype, see Fig. 8I,J. However, no such direct link had been made between the male tail phenotype and cell cycle defects. To test whether the *mat-1* male tail defects (Fig. 8A-D) also correlated with mitotic cell cycle defects, L1 larvae from either the severely affected *ax144; him-8* strain or *him-8* controls were shifted to 25.5°C for periods ranging from 18 to 36 hours. The animals were dissected to separate the gonad from the soma, and then processed for immunostaining with anti-p-H3 antibody. The somatic staining patterns in the *ax144* samples were indistinguishable from the controls during the 18- and 24-hour time points. However, a dramatic excess of p-H3 staining cells was found in the posterior of *ax144* L4 male larvae collected 30 to 36 hours (L4) after upshift (Fig. 8H,K) when compared to the wild-type controls (Fig. 8F,K). Importantly, only some of these p-H3-positive cells were in metaphase, suggesting that the APC/C defect is prolonging more than just the metaphase to anaphase transition. Because both the final cell divisions and morphogenetic events of male tail formation occur during this same L4 period, it is likely that at least some of these p-H3-positive cells were progenitors of male tail cells. Thus, as in the vulva, the morphological defects in the mutant male tails are likely to stem from a combination of M-phase delays and potential truncations within these late-dividing cell lineages.

Table 5. Double mutants reveal germline defects in *mat-1* mutants

	mat-1(ax227) 15°C	*mat-1(ax227)* 25°C	*mat-1(ax212)* 15°C
mat-2(or170) apc-1*	Mel	Mel	Fertile
mat-3(ax148) *cdc-23/apc-8**	Mel	Sterile	Fertile
mat-3(or180) *cdc-23/apc-8**	Mel	Sterile	Mel; Sterile
emb-27(g48) *cdc-16/apc-6*†*	Fertile	Mel	Fertile
emb-30(g53) *apc-4*‡*	Mel	Sterile	Mel

Double mutants were constructed as described in the Materials and Methods. In 25ºC analysis, candidate *mat-1/+; mat-x/+* or *mat-1/+*; *emb-x/+* animals were shifted from 15ºC to 25ºC as either embryos or L1 larvae. Mel, maternal-effect embryonic lethality in which homozygous mothers from heterozygous parents produce clutches of dead embryos.

For molecular cloning results see *Davis et al., 2002, †Golden et al., 2000, ‡Furuta et al., 2000.

DISCUSSION

The APC/C is widely recognized as the key E3 ubiquitin ligase that drives cells through and subsequently out of mitosis (Peters, 2002). In the present study, we have employed *C. elegans* temperature-sensitive mutants in the APC/C subunit MAT-1/CDC-27 to reveal a wide range of defects at both the organ and cellular level that can result from partial depletions of APC/C activity. When MAT-1 was significantly depleted by either shifting *mat-1(ts)* mothers to 25.5°C or injecting wild-

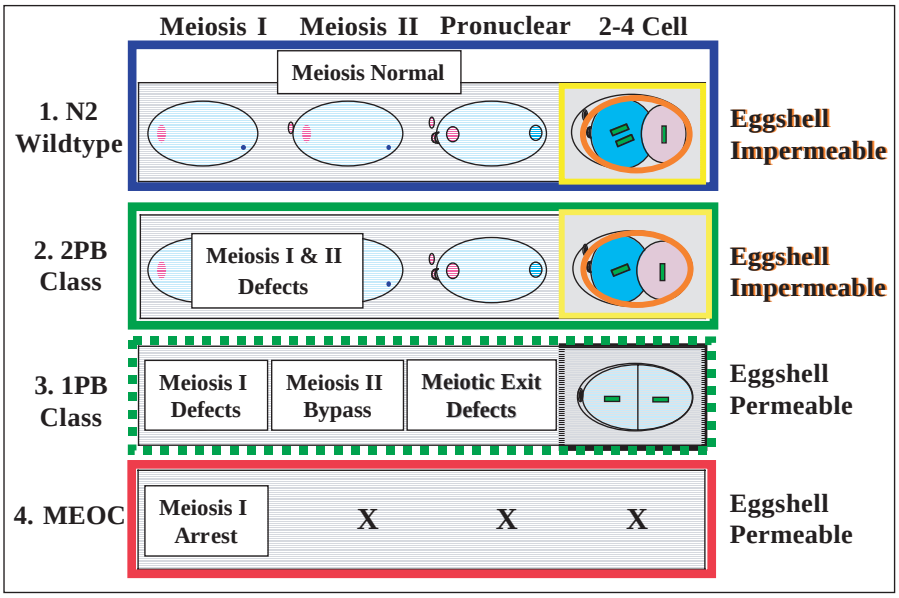

Fig. 9. Summary of meiotic and developmental defects observed in *mat-1* hypomorphs. Under semi-permissive temperatures (rows 1-3), three different classes of meiotic and developmental phenotypes are observed for *mat-1* mutants: normal meiosis (top row), the 2PB class (row 2), and the 1PB class (row 3). In the 2PB class, both MI and MII defects occur, leading to asymmetric but more synchronous divisions in the two- to four-cell stage. In the 1PB class, MI defects occur, MII is skipped, and meiotic exit defects are apparent. These defects lead to a symmetric first cleavage and a synchronous second mitosis in which the orientations of divisions are abnormal. Eggshell formation is also defective. In the fully restrictive conditions (row 4), all embryos arrest at metaphase of MI and make weak, incompletely hardened eggshells.

type mothers with double-stranded *mat-1/cdc-27* RNA, the affected oocytes were fertilized but arrested as one-cell embryos with their paired homologs locked in metaphase of meiosis I. In contrast, when various temperature shift regimes were used to create a graded MAT-1 depletion series, the resulting one-cell embryos exhibited an extended meiotic phase as well as several dosage-dependent meiotic defects ranging from incomplete chromosome separation and abnormal meiotic spindle dynamics to a complete bypass of the second meiotic division. While metaphase I-arrested *mat-1* embryos exhibit a corresponding developmental block at the meiotic one-cell stage, hypomorphic *mat-1* embryos exhibited dosage-dependent meiotic defects that correlated with specific defects in early development (Fig. 9). These developmental defects included altered pronuclear migration patterns, aberrant polarization, and alterations in the normal timing and orientation of the embryo's mitotic cell divisions. When *mat-1* mutants were upshifted as L1 larvae, additional somatic and germline defects were observed in three of the seven alleles; other alleles could be induced to exhibit these phenotypes in double mutant combinations with other APC/C subunits.

Structure/function analysis

Sequence analysis of the seven mutant alleles revealed molecular lesions predominantly within the TPR domains but otherwise scattered throughout the *mat-1* coding region, and our subsequent phenotypic analysis revealed no obvious correlation between the location of these lesions and the severity of the mutant defects. In particular, the mutations in two phenotypically similar alleles, *ax161* and *ax227*, are well separated within the linear sequence of MAT-1 whereas two phenotypically dissimilar, alleles, *ax520* and *ax212*, are almost adjacent. These results combined with the previous findings that Mat embryos contain sufficient functional, maternal APC/C to develop into sterile adults even when upshifted to 25°C as two-cell embryos (Golden et al., 2000), suggest that all of these alleles, except *ax72* and *ax520*, are temperature sensitive for protein folding. In such mutants, high temperatures destabilize an intermediate in the folding pathway without altering the functions of the folded state (King et al., 1996). None of the seven *mat-1* alleles are molecular nulls, however, we believe that the *mat-1* metaphase I arrest phenotype reflects an absence of APC/C function within the oocyte since RNAi embryos of seven different APC/C subunits display an identical phenotype (this study) (Davis et al., 2002). Contrary to our initial expectations, none of these *mat-1* alleles, except perhaps *ax72*, proved to be meiotic specific. Perhaps mutations in TPR domains are poor candidates as single function lesions if the TPR domains in MAT-1/CDC-27 serve primarily to glue the complex together. Theoretically, mutations of phosphorylation sites might cause single function defects, but no such lesions are represented within our current mutant collection.

Tissue specificity of *C. elegans* cell cycle mutants

Although none of our *mat-1* alleles are molecular nulls, homozygous null embryos of other APC/C subunits survive embryogenesis and develop into sterile hermaphrodites with everted vulva [EMB-30/APC-4 (Furuta et al., 2000), MAT-2/APC-1 (Davis et al., 2002), MAT-3/CDC-23 (D. Garbe and M. Sundaram, personal communication), and APC-11 (A.G., unpublished)]. Furthermore, similar phenotypes have been described for null mutants of other cell cycle genes including cyclin D (Boxem and van den Heuvel, 2001; Park and Krause, 1999) cyclin E (Fay and Han, 2000) CDK-4 (Boxem and van den Heuvel, 2001; Park and Krause, 1999) and CDK-1 (Boxem et al., 1999). Presumably these cell cycle mutants survive embryogenesis and larval development because of high levels of persistent maternal mRNA or protein stores, and, in the case of temperature-sensitive mutants, the resistance of previously synthesized and complexed proteins to unfold at restrictive temperatures. The biology of *C. elegans* may also explain the surprisingly mild phenotypic defects. Since *C. elegans* embryos develop in the absence of net growth, maternal stores of cell cycle proteins may persist at sufficient concentrations to support cell divisions throughout embryogenesis. Likewise, surprisingly normal larval development can occur in the complete absence of larval cell divisions, albeit the resulting

adults are sterile and uncoordinated (Albertson et al., 1978). Similarly, many *Drosophila* cell cycle mutants (Gatti and Baker, 1989), including those in APC5 (Bentley et al., 2002) survive embryogenesis and larval development before dying during the prepupal stage with underdeveloped imaginal discs.

The germline, vulva, and male tail may be particularly sensitive to defects in the APC/C and other cell cycle genes because all three are generated through mitotic proliferation of embryonic blast cells, with the majority of divisions occurring during the last two larval stages. In the case of the germline, two germline progenitor cells proliferate more than any other blast cells in the hatching L1 larvae. The cell lineages giving rise to the developing male tail and hermaphrodite vulva do not involve more cell divisions than those giving rise to other somatic structures, but these divisions are sufficiently late that maternal stores may be inadequate. In addition, proper development of these organs requires a high degree of coordinated signaling interactions (Lambie, 2002) and thus may be particularly sensitive to M-phase delays and/or abnormalities that result in either truncation or altered timing of the cell lineages. Interestingly, *mat-1* mutants also exhibit gonad migration defects at low frequency (M.A. and D.S., unpublished), which may stem from cell signaling defects during gonadal development. Taken together, these studies suggest that, in multicellular organisms, the sensitivity of a particular tissue to hypomorphic APC/C levels will depend on total cell proliferation and the degree to which coordinated cell division is linked to morphogenesis.

Hypomorphic mutants reveal late and novel functions for the APC/C

APC/C dosage studies revealed a hierarchy of APC/C functions. Upon partial depletion of APC/C levels, chromosome separation is affected more than spindle shortening, and spindle shortening is more affected than either spindle rotation or polar body formation. A similar hierarchy has been observed in fission yeast; APC/C null mutants arrest in metaphase whereas most ts mutants exhibit a 'cut' phenotype in which cytokinesis proceeds in the absence of chromosome segregation (Chang et al., 2001). To date, the basis for this differential sensitivity remains unclear. In other systems, APC/C substrate specificity is regulated by its associated WD repeat proteins. Current models suggest that securin is targeted primarily by APC^{Cdc20} (Cohen-Fix et al., 1996; Funabiki et al., 1996b) whereas cyclin B is targeted primarily by APC^{Cdh1}, although recent studies suggest that the specific roles of these WD proteins may be more variable (Hsu et al., 2002; Sigrist and Lehner, 1997; Stegmeier et al., 2002; Yamaguchi et al., 2000; Yeong et al., 2000). Recent studies also indicate that $APC^{Cdc20/Fizzy}$ is the sole form of the APC/C during *C. elegans* meiosis; *fzy-1*(RNAi) embryos arrest in metaphase I (Kitagawa et al., 2002) whereas *cdh-1/fzr-1*(RNAi) embryos develop into sterile adults (Fay et al., 2002). If the CDH1/FZR-1 ortholog does not, in fact, function in meiotic *C. elegans* embryos, the observed hierarchy may reflect a differential affinity of APC^{Cdc20} for its various targets. Alternatively, if *C. elegans* has additional, yet undiscovered meiotic specificity factors (WD repeat proteins), perhaps only the higher affinity complexes function at low APC/C levels.

Our studies have also revealed a potentially novel APC/C function in late anaphase meiotic spindle shortening. In mitotic cells, APC/C contributes to changes in anaphase spindle morphology in part by ubiquitinating *Ase-1* (Juang et al., 1997; Visintin et al., 1997) and various kinesins (Gordon and Roof, 2001). Whether meiotic spindle shortening is directed through the same or unique APC/C substrates will be the subject of future studies.

APC/C may not be required for meiosis II exit

One of the more intriguing findings of this study was the differential effect that APC/C depletions had on the two meiotic divisions (Fig. 9). While partial depletions of APC/C activity disrupt the separation of paired homologs in MI and sister chromatids in MII, extended delays and/or arrest of the metaphase to anaphase transition occurred only during MI. While both the 1PB and 2PB class embryos experience extended MI delays, it was surprising that the MII chromosome separation defects in 2PB class embryos were never coupled with a metaphase II arrest or a prolonged MII cell cycle. One explanation for this result is that meiosis I is as sensitive, or more sensitive, than meiosis II to decreased APC/C activity, and thus it may not be possible experimentally to observe a MII arrest (since such temperatures result in a MI arrest). Alternatively, the differential impact reflects true differences between the two meiotic divisions. More specifically, oocytes normally transition between MI and MII without fully exiting M-phase; whereas exit from MII absolutely requires the destruction of M-phase cyclins and is accompanied by nuclear envelope reformation (Kobayashi et al., 1991; Minshull et al., 1991). While mitotically dividing cells drive M-phase with APC^{Cdh1} and the G1 to S transition with SCF (Deshaies, 1999), one-cell *C. elegans* embryos apparently lack a G1 stage and thus the final stages of MII exit in *C. elegans* and potentially other embryos could be driven not by the APC/C, but rather by SCF or another cullin/RING finger complex. Consistent with this model, RNAi depletion of a CUL-2-containing complex results in severe MII, but not MI, delays (E. Kipreos, personal communication).

The requirement for APC/C in A-P polarity is likely to be indirect

In previous studies, we and others have reported that complete and/or severe depletions of APC/C activity that block cell cycle progression past metaphase I also block the developmental processes of eggshell maturation (Golden et al., 2000) and the establishment of a stable A-P axis (Wallenfang and Seydoux, 2000). Subsequent analysis of separase, the cohesin-cleaving protease that is indirectly activated by APC^{Cdc20} activity, indicates that the depletion of separase activity alone is sufficient to block these two developmental events (Siomos et al., 2001; Rappleye et al., 2002) (this study). Importantly, our current results call into question the proposal that either the APC/C or separase function as direct regulators of either eggshell hardening or A-P polarization activity. In our APC/C and separase studies, defects in A-P polarization and eggshell hardening could only be generated under conditions in which the embryos exhibited severe meiotic defects (Fig. 9). In our more extensive APC/C dosage studies, not only did these 1PB class embryos fail to separate their homologs during metaphase I, but they skipped meiosis II altogether. More importantly, this drastic alteration in normal cell cycle progression disrupted the

normally clean transition from meiosis to zygotic S phase. Notable defects include slow disassembly of the meiotic spindle and delayed maturation of the sperm asters. Given that the polarity machinery is thought to cue on microtubule free-ends (Wallenfang and Seydoux, 2000), the co-existence and aberrant placement of these two microtubule structures might be sufficient to disrupt polarity. Although our studies cannot specifically rule out a direct connection between separase function and polarity, the observed transition defects provide an explanation of the APC/C-associated polarity defects that does not require the existence of novel, non-cell cycle roles for the APC/C and/or separase.

We would like to thank Yuji Kohara (National Institute of Genetics, Japan) for providing *cdc-27* cDNA clones, Matt Wallenfang and Geraldine Seydoux for the *cdc-27* RNAi feeding construct, Raffi Aroian for the *ye121* allele, Judith Austin for the integrated histone H2B::GFP fusion transgenic line, the *C. elegans* Genetics Center (University of Minnesota), funded by the NIH National Center for Research Resources, for providing strains, and Michael Krause and Thomas Brodigan for assistance with sequencing. We also are grateful to Meera Sundaram, Risa Kitagawa, Ann Rose and Edward Kipreos for sharing unpublished data. Special thanks go to Barry Chestnut and James LaRue for technical assistance, and Lizabeth Allison, Orna Cohen-Fix, April Robbins, Ritu Argawal, Karen Ross, Edward Davis, Barry Chestnut, Kevin O'Connell, Geraldine Seydoux, and members of the Bethesda/DC Worm Club for feedback and advice during the course of these studies. This work was supported in part by NIH grant GM060359-01 (to D.C.S.) and a College of William and Mary Faculty Research Assignment Grant (to D.C.S.).

REFERENCES

Abrieu, A., Doree, M. and Fisher, D. (2001). The interplay between cyclin-B-Cdc2 kinase (MPF) and MAP kinase during maturation of oocytes. *J. Cell Sci.* **114**, 257-267.

Albertson, D. G. (1984). Formation of the first cleavage spindle in nematode embryos. *Dev. Biol.* **101**, 61-72.

Albertson, D. G., Sulston, J. E. and White, J. G. (1978). Cell cycling and DNA replication in a mutant blocked in cell division in the nematode *Caenorhabditis elegans*. *Dev. Biol.* **63**, 165-178.

Albertson, D. G. and Thomson, J. N. (1993). Segregation of holocentric chromosomes at meiosis in the nematode, *Caenorhabditis elegans*. *Chrom. Res.* **1**, 15-26.

Asakawa, H., Kitamura, K. and Shimoda, C. (2001). A novel Cdc20-related WD-repeat protein, Fzr1, is required for spore formation in Schizosaccharomyces pombe. *Mol. Genet. Genomics* **265**, 424-435.

Bentley, A. M., Williams, B. C., Goldberg, M. L. and Andres, A. J. (2002). Phenotypic characterization of Drosophila ida mutants: defining the role of APC5 in cell cycle progression. *J. Cell Sci.* **115**, 949-961.

Blanco, M. A., Pelloquin, L. and Moreno, S. (2001). Fission yeast mfr1 activates APC and coordinates meiotic nuclear division with sporulation. *J. Cell Sci.* **114**, 2135-2143.

Boxem, M., Srinivasan, D. G. and van den Heuvel, S. (1999). The *Caenorhabditis elegans* gene *ncc-1* encodes a cdc2-related kinase required for M phase in meiotic and mitotic cell divisions, but not for S phase. *Development* **126**, 2227-2239.

Boxem, M. and van den Heuvel, S. (2001). lin-35 Rb and cki-1 Cip/Kip cooperate in developmental regulation of G1 progression in *C. elegans*. *Development* **128**, 4349-4359.

Castro, A., Arlot-Bonnemains, Y., Vigneron, S., Labbe, J. C., Prigent, C. and Lorca, T. (2002). APC/Fizzy-related targets Aurora-A kinase for proteolysis. *EMBO Rep.* **3**, 457-462.

Chang, L., Morrell, J. L., Feoktistova, A. and Gould, K. L. (2001). Study of cyclin proteolysis in anaphase-promoting complex (APC) mutant cells reveals the requirement for APC function in the final steps of the fission yeast septation initiation network. *Mol. Cell. Biol.* **21**, 6681-6694.

Chitwood, B. G. and Chitwood, M. B. (1974). *Introduction to Nematology*. Baltimore: University Park Press.

Church, D. L., Guan, K. L. and Lambie, E. J. (1995). Three genes of the MAP kinase cascade, mek-2, mpk-1/sur-1 and let-60 ras, are required for meiotic cell cycle progression in *Caenorhabditis elegans*. *Development* **121**, 2525-2535.

Clandinin, T. R. and Mains, P. E. (1993). Genetic studies of *mei-1* gene activity during the transition from meiosis to mitosis in *Caenorhabditis elegans*. *Genetics* **134**, 199-210.

Cohen-Fix, O., Peters, J. M., Kirschner, M. W. and Koshland, D. (1996). Anaphase initiation in Saccharomyces cerevisiae is controlled by the APC-dependent degradation of the anaphase inhibitor Pds1p. *Genes Dev.* **10**, 3081-3093.

Cooper, K. F., Mallory, M. J., Egeland, D. B., Jarnik, M. and Strich, R. (2000). Ama1p is a meiosis-specific regulator of the anaphase promoting complex/cyclosome in yeast. *Proc. Natl. Acad. Sci. USA* **97**, 14548-14553.

Davis, E. S., Wille, L., Chestnut, B. A., Sadler, P. L., Shakes, D. C. and Golden, A. (2002). Multiple subunits of the *Caenorhabditis elegans* Anaphase-Promoting Complex are required for chromosome segregation during meiosis I. *Genetics* **160**, 805-813.

Deshaies, R. J. (1999). SCF and Cullin/Ring H2-based ubiquitin ligases. *Annu. Rev. Cell Dev. Biol.* **15**, 435-467.

Edgar, L. G. (1995). Blastomere culture and analysis. In *Caenorhabditis elegans: Modern Biological Analysis of an Organism*, vol. 48 (ed. H. F. Epstein and D. C. Shakes), pp. 303-321. New York: Academic Press.

Fay, D. S. and Han, M. (2000). Mutations in cye-1, a *Caenorhabditis elegans* cyclin E homolog, reveal coordination between cell-cycle control and vulval development. *Development* **127**, 4049-4060.

Fay, D. S., Keenan, S. and Han, M. (2002). fzr-1 and lin-35/Rb function redundantly to control cell proliferation in C. elegans as revealed by a nonbiased synthetic screen. *Genes Dev.* **16**, 503-517.

Fire, A., Xu, S., Montgomery, M. K., Kostas, S. A., Driver, S. E. and Mello, C. C. (1998). Potent and specific genetic interference by double-stranded RNA in *Caenorhabditis elegans*. *Nature* **391**, 806-811.

Fraser, A. G., Kamath, R. S., Zipperlen, P., Martinez-Campos, M., Sohrmann, M. and Ahringer, J. (2000). Functional genomic analysis of *C. elegans* chromosome I by systematic RNA interference. *Nature* **408**, 325-330.

Funabiki, H., Kumada, K. and Yanagida, M. (1996a). Fission yeast Cut1 and Cut2 are essential for sister chromatid separation, concentrate along the metaphase spindle and form large complexes. *EMBO J.* **15**, 6617-6628.

Funabiki, H. and Murray, A. W. (2000). The Xenopus chromokinesin Xkid is essential for metaphase chromosome alignment and must be degraded to allow anaphase chromosome movement. *Cell* **102**, 411-424.

Funabiki, H., Yamano, H., Kumada, K., Nagao, K., Hunt, T. and Yanagida, M. (1996b). Cut2 proteolysis required for sister-chromatid separation in fission yeast. *Nature* **381**, 438-441.

Furuta, T., Tuck, S., Kirchner, J., Koch, B., Auty, R., Kitagawa, R., Rose, A. M. and Greenstein, D. (2000). EMB-30: an APC4 homologue required for metaphase-to-anaphase transitions during meiosis and mitosis in Caenorhabditis elegans. *Mol. Biol. Cell* **11**, 1401-1419.

Gatti, M. and Baker, B. S. (1989). Genes controlling essential cell-cycle functions in Drosophila melanogaster. *Genes Dev.* **3**, 438-453.

Glover, D. M. (1989). Mitosis in Drosophila. *J. Cell Sci.* **92**, 137-146.

Golden, A., Sadler, P. L., Wallenfang, M. R., Schumacher, J. M., Hamill, D. R., Bates, G., Bowerman, B., Seydoux, G. and Shakes, D. C. (2000). Metaphase to anaphase (*mat*) transition-defective mutants in *Caenorhabditis elegans*. *J. Cell Biol.* **151**, 1469-1482.

Goldstein, B. and Hird, S. N. (1996). Specification of the anteroposterior axis in *Caenorhabditis elegans*. *Development* **122**, 1467-1474.

Gordon, D. M. and Roof, D. M. (2001). Degradation of the kinesin Kip1p at anaphase onset is mediated by the anaphase-promoting complex and Cdc20p. *Proc. Natl. Acad. Sci. USA* **98**, 12515-12520.

Gotta, M. and Ahringer, J. (2001). Axis determination in C. elegans: initiating and transducing polarity. *Curr. Opin. Genet. Dev.* **11**, 367-373.

Harper, J. W., Burton, J. L. and Solomon, M. J. (2002). The anaphase-promoting complex: it's not just for mitosis any more. *Genes Dev.* **16**, 2179-2206.

Hershko, A. and Ciechanover, A. (1998). The ubiquitin system. *Annu. Rev. Biochem.* **67**, 425-479.

Hirsh, D., Oppenheim, D. and Klass, M. (1976). Development of the reproductive system of *Caenorhabditis elegans*. *Dev. Biol.* **49**, 200-219.

Hodgkin, J. T., Horvitz, H. R. and Brenner, S. (1979). Nondisjunction mutants of the nematode *Caenorhabditis elegans*. *Genetics* **91**, 67-94.

Hsu, J. Y., Reimann, J. D., Sorensen, C. S., Lukas, J. and Jackson, P. K. (2002). E2F-dependent accumulation of hEmi1 regulates S phase entry by inhibiting APC(Cdh1). *Nat. Cell Biol.* **4**, 358-366.

Hunter, C. P. (1999). Genetics: a touch of elegance with RNAi. *Curr. Biol.* **9**, R440-442.

Juang, Y. L., Huang, J., Peters, J. M., McLaughlin, M. E., Tai, C. Y. and Pellman, D. (1997). APC-mediated proteolysis of Ase1 and the morphogenesis of the mitotic spindle. *Science* **275**, 1311-1314.

King, J., Haase-Pettingell, C., Robinson, A. S., Speed, M. and Mitraki, A. (1996). Thermolabile folding intermediates: inclusion body precursors and chaperonin substrates. *FASEB J.* **10**, 57-66.

King, R. W., Jackson, P. K. and Kirschner, M. (1994). Mitosis in transition. *Cell* **79**, 563-571.

Kitagawa, R., Law, E., Tang, L. and Rose, A. M. (2002). The Cdc20 homolog, FZY-1, and its interacting protein, IFY-1, are required for proper chromosome segregation in *Caenorhabditis elegans*. *Curr. Biol.* **12**, 2118-2123.

Kobayashi, H., Minshull, J., Ford, C., Golsteyn, R., Poon, R. and Hunt, T. (1991). On the synthesis and destruction of A- and B-type cyclins during oogenesis and meiotic maturation in Xenopus laevis. *J. Cell Biol.* **114**, 755-765.

Lamb, J. R., Tugendreich, S. and Hieter, P. (1995). Tetratrico peptide repeat interactions: to TPR or not to TPR? *Trends Biochem. Sci.* **20**, 257-259.

Lambie, E. J. (2002). Cell proliferation and growth in C. elegans. *BioEssays* **24**, 38-53.

Lyczak, R., Gomes, J. E. and Bowerman, B. (2002). Heads or tails: cell polarity and axis formation in the early Caenorhabditis elegans embryo. *Dev. Cell* **3**, 157-166.

McCarter, J., Bartlett, B., Dang, T. and Schedl, T. (1999). On the control of oocyte meiotic maturation and ovulation in *Caenorhabditis elegans*. *Dev. Biol.* **205**, 111-128.

McCollum, D. and Gould, K. L. (2001). Timing is everything: regulation of mitotic exit and cytokinesis by the MEN and SIN. *Trends Cell Biol.* **11**, 89-95.

Minshull, J., Murray, A., Colman, A. and Hunt, T. (1991). Xenopus oocyte maturation does not require new cyclin synthesis. *J. Cell Biol.* **114**, 767-772.

Morgan, D. O. (1999). Regulation of the APC and the exit from mitosis. *Nat. Cell Biol.* **1**, E47-53.

O'Connell, K. F., Maxwell, K. N. and White, J. G. (2000). The spd-2 gene is required for polarization of the anteroposterior axis and formation of the sperm asters in the *Caenorhabditis elegans* zygote. *Dev. Biol.* **222**, 55-70.

Park, M. and Krause, M. W. (1999). Regulation of postembryonic G(1) cell cycle progression in *Caenorhabditis elegans* by a cyclin D/CDK-like complex. *Development* **126**, 4849-4860.

Pellettieri, J. and Seydoux, G. (2002). Anterior-posterior polarity in *C. elegans* and *Drosophila*–PARallels and differences. *Science* **298**, 1946-1950.

Peter, M., Castro, A., Lorca, T., le Peuch, C., Magnaghi-Jaulin, L., Doree, M. and Labbe, J. C. (2001). The APC is dispensable for first meiotic anaphase in Xenopus oocytes. *Nat. Cell Biol.* **3**, 83-87.

Peters, J. M. (2002). The anaphase-promoting complex: proteolysis in mitosis and beyond. *Mol. Cell* **9**, 931-943.

Praitis, V., Casey, E., Collar, D. and Austin, J. (2001). Creation of low-copy integrated transgenic lines in *Caenorhabditis elegans*. *Genetics* **157**, 1217-1226.

Rappleye, C. A., Tagawa, A., Lyczak, R., Bowerman, B. and Aroian, R. V. (2002). The anaphase-promoting complex and separin are required for embryonic anterior-posterior axis formation. *Dev. Cell* **2**, 195-206.

Sadler, P. L. and Shakes, D. C. (2000). Anucleate *Caenorhabditis elegans* sperm can crawl, fertilize oocytes and direct anterior-posterior polarization of the 1-cell embryo. *Development* **127**, 355-366.

Sigrist, S. J. and Lehner, C. F. (1997). Drosophila *fizzy-related* down-regulates mitotic cyclins and is required for cell proliferation arrest and entry into endocycles. *Cell* **90**, 671-681.

Siomos, M. F., Badrinath, A., Pasierbek, P., Livingstone, D., White, J., Glotzer, M. and Nasmyth, K. (2001). Separase is required for chromosome segregation during meiosis I in *Caenorhabditis elegans*. *Curr. Biol.* **11**, 1825-1835.

Stegmeier, F., Visintin, R. and Amon, A. (2002). Separase, polo kinase, the kinetochore protein Slk19, and Spo12 function in a network that controls Cdc14 localization during early anaphase. *Cell* **108**, 207-220.

Stroschein, S. L., Bonni, S., Wrana, J. L. and Luo, K. (2001). Smad3 recruits the anaphase-promoting complex for ubiquitination and degradation of SnoN. *Genes Dev.* **15**, 2822-2836.

Sulston, J. E. and Horvitz, H. R. (1977). Post-embryonic cell lineages of the nematode, *Caenorhabditis elegans*. *Dev. Biol.* **56**, 110-156.

Taguchi, S., Honda, K., Sugiura, K., Yamaguchi, A., Furukawa, K. and Urano, T. (2002). Degradation of human Aurora-A protein kinase is mediated by hCdh1. *FEBS Lett.* **519**, 59-65.

Taieb, F. E., Gross, S. D., Lewellyn, A. L. and Maller, J. L. (2001). Activation of the anaphase-promoting complex and degradation of cyclin B is not required for progression from Meiosis I to II in Xenopus oocytes. *Curr. Biol.* **11**, 508-513.

Timmons, L., Court, D. L. and Fire, A. (2001). Ingestion of bacterially expressed dsRNAs can produce specific and potent genetic interference in Caenorhabditis elegans. *Gene* **263**, 103-112.

Uhlmann, F., Lottspeich, F. and Nasmyth, K. (1999). Sister-chromatid separation at anaphase onset is promoted by cleavage of the cohesin subunit Scc1. *Nature* **400**, 37-42.

Uhlmann, F., Wernic, D., Poupart, M. A., Koonin, E. V. and Nasmyth, K. (2000). Cleavage of cohesin by the CD clan protease separin triggers anaphase in yeast. *Cell* **103**, 375-386.

Vidwans, S. J. and Su, T. T. (2001). Cycling through development in Drosophila and other metazoa. *Nat. Cell Biol.* **3**, E35-39.

Visintin, R., Prinz, S. and Amon, A. (1997). CDC20 and CDH1: a family of substrate-specific activators of APC-dependent proteolysis. *Science* **278**, 460-463.

Wallenfang, M. R. and Seydoux, G. (2000). Polarization of the anterior-posterior axis of *C. elegans* is a microtubule-directed process. *Nature* **408**, 89-92.

Wan, Y., Liu, X. and Kirschner, M. W. (2001). The anaphase-promoting complex mediates TGF-beta signaling by targeting SnoN for destruction. *Mol. Cell* **8**, 1027-1039.

Yamaguchi, S., Okayama, H. and Nurse, P. (2000). Fission yeast Fizzy-related protein srw1p is a G(1)-specific promoter of mitotic cyclin B degradation. *EMBO J.* **19**, 3968-3977.

Yeong, F. M., Lim, H. H., Padmashree, C. G. and Surana, U. (2000). Exit from mitosis in budding yeast: biphasic inactivation of the Cdc28-Clb2 mitotic kinase and the role of Cdc20. *Mol. Cell* **5**, 501-511.

Zipperlen, P., Fraser, A. G., Kamath, R. S., Martinez-Campos, M. and Ahringer, J. (2001). Roles for 147 embryonic lethal genes on *C. elegans* chromosome I identified by RNA interference and video microscopy. *EMBO J.* **20**, 3984-3992.